8-2012

DIRECT EFFECTS OF METFORMIN ON PI3K AND RAS SIGNALING IN ENDOMETRIAL CANCER

David A. Iglesias M.D.

DIRECT EFFECTS OF METFORMIN ON PI3K AND RAS SIGNALING IN ENDOMETRIAL CANCER

By

David A. Iglesias, M.D.

APPROVED:

Karen H. Lu, M.D.

Supervisory Professor

Rosemarie Schmandt, Ph.D.

Russell Broaddus, M.D., Ph.D.

Samuel Mok, Ph.D.

Kwong K. Wong, Ph.D.

George Stancel, Ph.D.

Dean, Graduate School of Biomedical Sciences

The University of Texas Health Science Center at Houston

DIRECT EFFECTS OF METFORMIN ON PI3K AND RAS SIGNALING IN ENDOMETRIAL CANCER

A

THESIS

Presented to the Faculty of

The University of Texas

Health Science Center at Houston

and

The University of Texas

M.D. Anderson Cancer Center

Graduate School of Biomedical Sciences

In Partial Fulfillment

of the Requirements

for the Degree of

MASTERS OF SCIENCE

by

David A. Iglesias, M.D.

Houston, TX

August 2012

DEDICATIONS

To my wife, Jeniffer, and my two kids, Sophia and Jonah, for all of your love, patience, and encouragement. You all have been the greatest gift that God has given me. I am truly blessed to have you all in my life.

To my parents, Jesus and Ana, for your tireless support and guidance throughout the years. A son could not have asked for better parents – thank you.

ACKNOWLEDGEMENTS

First and foremost, I would like to thank my Lord and Savior Jesus Christ without whom none of this would have been possible.

There are so many people who have been instrumental to this research and to my education. Dr. Karen Lu has been a thoughtful, honest, and patient thesis advisor and mentor. Thank you for your willingness to have me as a member of your lab, the many projects that you allowed me to be a part of, the many times you allowed me to barge into your office to discuss results and ideas, and your continued support of my career.

To the past and present members of the Lu Lab – I cannot say "thank you" enough for all of your help. Specifically, I thank Qian Zhang, Chloe Co, Melinda Yates, Joseph Celestino, Jessica Bowser, Jennifer Burzawa, Marilyn Huang, Tri Nguyen, and Connie Teodoro for all their expertise and knowledge that they handed down to me over the course of the last couple of years – there is no way I could have completed these experiments without your help and insights.

I would also like to acknowledge and thank those who have served on my advisory and supervisory committees: Dr. Russell Broaddus, Dr. Kwong K. Wong, Dr. Samuel Mok, Dr. Rosie Schmandt, and Dr. Karen Lu. I have enjoyed hearing your feedback and sincerely appreciate your encouragement in moving this project forward. Thank you for your reassurance and wisdom. Specifically, Dr. Rosie Schmandt, whose excitement about research, mice, and proteins is infectious. Thank you for taking something that I knew very little about and getting me hooked

and wanting more, only to come to the realization that there is still so much more to learn.

Thank you to Dr. John Hancock and his lab members - Travis Rodkey, Dharini Van der Hoeven, and Sravanthi Chigurupati - at the University of Texas Medical School at Houston for all of their expertise and help in performing the Ras trafficking and confocal imaging studies.

There are several other collaborators that I would also like to acknowledge. Thank you to Dr. Francesco DeMayo and Dr. Jae-Wook Jeong for providing the transgenic mouse from which we derived the MecPK cell line. Thank you to Dr. Kwong K. Wong, Dr. Samuel Mok, and Dr. Gordon Mills whose labs at one point or another provided invaluable insight and resources that assisted me in completing these studies. Thank you to the members of the Flow Cytometry Core facility for their assistance and expertise. Thank you to the veterinarians and animal care technicians who tirelessly cared for our mice.

Thank you to my co-fellows and friends – Erin King and Justin Bottsford-Miller – for their ability to listen and provide a fresh set of eyes. I look forward to working with you both for many years to come.

Over the course of the last couple of years, I have quickly come to the realization that any successful project requires input from many dedicated individuals and teams – thank you all.

The project described was supported by Grant Number T32 CA101642 from the NIH National Research Service Award. Its contents are solely the responsibility of the authors and do not necessarily represent the official views of the NIH.

DIRECT EFFECTS OF METFORMIN ON PI3K AND RAS SIGNALING IN ENDOMETRIAL CANCER

David A. Iglesias, M.D.

Thesis Advisor: Karen H. Lu, M.D.

Metformin has antiproliferative effects through the activation of AMPK and has gained interest as an antineoplastic agent in several cancer types, although studies in endometrial cancer (EC) are limited. The aims of this project were to evaluate pathways targeted by metformin in EC, investigate mechanisms by which metformin exerts its antiproliferative effects, and explore rational combination therapies with other targeted agents.

Three EC cell lines were used to evaluate metformin's effect on cell proliferation, PI3K and Ras-MAPK signaling, and apoptosis. A xenograft mouse model was also used to evaluate the effects of metformin treatment on *in vivo* tumor growth. These preliminary studies demonstrated that K-Ras mutant cell lines exhibited a decreased proliferative rate, reduced tumor growth, and increased apoptosis in response to metformin compared to K-Ras wild-type cells.

To test the hypothesis that mutant K-Ras may predict response to metformin, murine EC cells with loss of PTEN and expressing mutant K-RasG12D were transfected to re-express PTEN or have K-Ras silenced using siRNA. While PTEN expression did not alter response to metformin, cells in which K-Ras was silenced displayed reduced sensitivity to metformin.

Mislocalization of K-Ras to the cytoplasm is associated with decreased signaling and induction of apoptosis. Metformin's effect on K-Ras localization was analyzed by confocal microscopy in cells expressing oncogenic GFP-K-RasG12V. Metformin demonstrated concentration-dependent mislocalization of K-Ras to the cytoplasm. Mislocalization of K-Ras to the cytoplasm was confirmed in K-Ras mutant EC cells (Hec1A) by cell fractionation in response to metformin 1 and 5 mM ($p=0.008$ and $p=0.004$). This effect appears to be AMPK-independent as combined treatment with Compound C, an AMPK inhibitor, did not alter K-Ras localization. Furthermore, treatment of EC cells with metformin in combination with PI3K inhibitors resulted in a significant decrease in proliferation than either agent or metformin alone.

While metformin exerts antineoplastic effects by activation of AMPK and decreased PI3K signaling, our data suggest that metformin may also disrupt localization of K-Ras and hence its signaling in an AMPK-independent manner. This has important implications in defining patients who may benefit from metformin in combination with other targeted agents, such as mTOR inhibitors.

TABLE OF CONTENTS

LIST OF ILLUSTRATIONS

LIST OF TABLES

1. Introduction

1.1. Overview

Metformin is one of the most widely prescribed oral hypoglycemic agents in the treatment of type II diabetes mellitus. The American Diabetes Association and the European Association for the Study of Diabetes both recommend metformin as the initial pharmacologic therapy for type II diabetes when lifestyle modifications fail (1). Benefits to its use include that it is generally well tolerated with minimal or rare adverse effects, cost is low, it is widely available, and is rarely associated with hypoglycemia. Recently, the use of metformin has gained interest in cancer research by demonstrating antineoplastic effects that are independent of its hypoglycemic effects (2). Furthermore, several clinical studies have demonstrated the association between metformin and an improvement in cancer incidence and survival (3-12). However, there has been limited data on the role of metformin specifically on endometrial cancer and the studies that have been performed have been limited to cell culture. As such, we sought to evaluate the effect of metformin on endometrial cancer *in vitro* and *in vivo* and to identify specific genetic alterations that may make cancer cells more susceptible to metformin treatment.

1.2. History of Metformin

Metformin and other biguanides were derived from guanidine found in *Galega officinalis*, otherwise known as goat's rue or French lilac. This plant was used as a treatment for polyuria related to diabetes in medieval Europe (13). It was not until the early 20th century that guanidine was described as the active compound and was synthesized for widespread use as an oral hypoglycemic agent. Metformin was first

described in 1922 by Emil Werner and James Bell as a product of the synthesis of N,N-dimethylguanidine (14). Previously, in 1918, guanidine was found to demonstrate hypoglycemic activity in animals (15). Unfortunately, guanidines were determined to be too toxic and attention shifted to a less toxic extract of *G. officinalis* called galegine (isoamylene guanidine) (16). Galegine and its analogs, the synthalins, were used sporadically in the 1920s as antidiabetic agents. However, as a result of the increasing availability of insulin in the 1920s and a better understanding of the pathophysiology of diabetes, interest in the oral agents waned. It wasn't until the 1940s and 50s that guanidines resurfaced primarily as agents to combat infections. Chloroguanidine hydrochloride was being used in the 1940s as an antimalarial agent when it was shown to also have a glucose-lowering effect (17). Around the same time, a prominent Philippine physician named Eusebio Garcia used a preparation of dimethyl biguanide, which he termed Flumamine, to treat influenza. He published his report in 1950 and noted that Flumamine was non-toxic and was associated with a lowering of serum glucose levels (18). Meanwhile, Jean Sterne, a French physician interested in diabetology, was conducting studies using galegine in Paris. Based partially on the observations by Eusebio Garcia, Sterne began exploring the antidiabetic properties of dimethyl biguanide, a compound he later called "Glucophage" (16). Sterne went on to publish his findings in 1957 (19). Shortly following this, others published trials with the biguanides phenformin and buformin (16). Although, both phenformin and buformin were initially considered more potent than metformin, they quickly fell out of favor due to their higher association with lactic acidosis and were ultimately discontinued in the 1970s. In

contrast, metformin became available in the United Kingdom in 1958 and was approved for use in Canada in 1972. Metformin was not approved by the U.S. Food and Drug Administration for Type II diabetes mellitus until 1994. Glucophage was later produced under license by Bristol-Myers Squibb in the U.S. beginning in March 1995. Several generic formulations currently exist.

1.3. Proposed Mechanisms of Metformin Action in Normal and Neoplastic Tissues

The principle mechanisms of action of metformin in the management of diabetes mellitus include reducing hepatic gluconeogenesis, increasing insulin sensitivity in target tissues, and improving glucose uptake by skeletal muscle and adipocytes (20). These actions ultimately lead to decreased circulating glucose and insulin levels. Specifically, metformin has been shown to inhibit mitochondrial respiratory chain complex I resulting in decreased adenosine-5'-triphosphate (ATP) generation (21), an increase in the AMP to ATP ratio, and subsequent activation of the cellular energy-sensing liver kinase B-1 (LKB1) and AMP-activated protein kinase (AMPK) pathway. AMPK activation results in the downregulation of energy-consuming processes such as lipid and protein synthesis in response to energy depletion. In the case of hepatocytes, this results in a decrease in gluconeogenesis and promotes glucose uptake. Glucose can be utilized by cells to generate ATP through oxidative phophorylation or glycolysis. However, following the observations that insulin acts as a mitogen in a subset of cancer cells (22) and that AMPK activation also inhibits mammalian target of rapamycin (mTOR) signaling, a pathway involved in cellular

proliferation and mRNA translation, there has been increasing interest in evaluating the potential direct antineoplastic effects of metformin.

It has been proposed that metformin exerts its antineoplastic effects through one or more of three mechanisms, some of which overlap with the mechanisms of action of metformin in normal tissues (23). In the “indirect” model, the action of metformin on hepatocytes results in decreased hepatic glucose secretion and increased glucose uptake. This ultimately leads to decreased circulating glucose and insulin levels. As insulin acts as a mitogen in a subset of cancers, a reduction in serum insulin levels may lead to a reduced growth rate of these tumors. However, it has been proposed that this mechanism would primarily benefit patients with baseline hyperinsulinemia, tumors that are insulin sensitive, and/or tumors lacking an activating mutation downstream of the insulin receptor (24). While metformin’s activation of the LKB1/AMPK pathway in hepatocytes results in decreased gluconeogenesis, several early studies also demonstrated that metformin had a similar “direct” effect on the LKB1/AMPK pathway in cancer cells, including breast, prostate, colon, and endometrial cancer cell lines. The end product of activation of LKB1/AMPK in these cells is inhibition of mTOR signaling resulting in decreased protein synthesis and reduced tumor growth (25-27). Evidence also indicates that metformin may inhibit growth of certain tumors by causing a cellular “energy crisis.” In this proposed model, tumors with loss of LKB1 or p53 are unable to sense, and therefore compensate for, a metformin-induced reduction in ATP resulting in a continuation of energy-consuming processes that ultimately leads to an energy crisis

and necrotic cell death (23, 28). Despite ongoing research, the precise mechanism(s) of metformin's antineoplastic activity has yet to be fully defined.

Metformin has also been shown to exhibit cardioprotective effects both *in vitro* and *in vivo* through increasing expression of AMPK and endothelial nitric oxide synthase (eNOS) and decreasing expression of transforming growth factor (TGF)-β1 in cardiomycotes leading to improved left ventricular function and modeling (29, 30). Furthermore, metformin use is also associated with a reduction in fatty acid levels and consequently an improvement in lipid profiles. These actions have translated to an improvement in survival in a murine model of heart failure (31). In humans, the United Kingdom Prospective Diabetes Study Group demonstrated that patients with type II diabetes who used metformin had a 36% decrease in all-cause mortality and a 39% lower risk of myocardial infarction when compared to other standard treatments (32). As a result of these findings, there are several ongoing clinical studies evaluating the role of metformin as a cardioprotective agent (33). These potential cardioprotective effects may contribute to the improvement in survival seen in epidemiological studies involving cancer patients.

1.4. Pharmacokinetics of Metformin

The ability of metformin to exert its antidiabetic and antineoplastic effects depends greatly on the ability of the drug to access and be taken up by the target tissue. Metformin exists primarily as a hydrophilic cationic molecule at physiologic pH levels resulting in low lipid solubility and very limited passive diffusion through cell membranes (34). As a result, uptake of metformin is largely mediated by organic cation transporters (OCTs), which are briefly reviewed below. Metformin is

predominantly absorbed from the small intestine through the activity of several transporters, notably the plasma membrane monoamine transporter (PMAT) which is found on the luminal surface of enterocytes (35). Peak plasma concentrations of metformin occur approximately 3 hours after a single oral dose of an immediate-release tablet (36). After multiple doses of 1000 mg twice daily, mean plasma concentrations of metformin range between 0.4 and 1.3 mg/L (37). The mean half-life is 5.1 hours in healthy patients with adequate renal function (37). The mean bioavailability of metformin has been estimated as 55+/-16% (34); however, there appears to be some inter-subject variability which may be a result of differences in expression levels of transporters. Once in the circulation, metformin remains unbound to plasma proteins and has a large volume of distribution (estimated at approximately 300 L following 2000 mg daily dosing) likely attributable to considerable tissue uptake of the drug. Of note, in animal models, metformin concentrations several-fold higher than serum concentrations have been found in various tissue types (38, 39). The primary mode of elimination of metformin is through renal excretion of unchanged drug. As a result, the elimination of metformin decreases with worsening renal function. The estimated mean renal clearance is 507+/-129 mL/min in healthy subjects with adequate renal function (34). Although approximately 20-30% of metformin is recovered in the feces following oral administration, this appears to be drug that was unabsorbed. Gastrointestinal elimination appears to be negligible as no drug has been found in feces following intravenous administration (36).

Transport of metformin from the plasma into target tissues is mediated by the activity of several OCTs, most notably OCT1 and OCT3. Both of these OCTs are found in many tissues and expressed at varying levels. As a major site of metformin activity, hepatocytes express high levels of both OCT1 and OCT3 (40). Supporting the importance of these transporters for metformin action, OCT1-knockout mice demonstrate decreased hepatic uptake of drug (41). Furthermore, transient silencing of OCT1 using siRNA decreased the sensitivity of epithelial ovarian cancer cells to metformin treatment (42). Animal studies have demonstrated that while OCT1 is primarily expressed in the liver, kidney, and small intestine it may also be expressed in other tissues to a lesser degree (40). In contrast, OCT3 appears to be strongly expressed in tissues of the female reproductive tract, notably the ovaries, placenta, and uterus (43). The high expression of OCTs in the kidneys likely explains their role in the elimination of metformin. Importantly, other basic drugs, such as cimetidine and certain antihistamines that are substrates for cation transporters, may decrease the renal clearance of metformin and vice versa.

1.5. Toxicities and Adverse Effects of Metformin

The most frequently reported adverse effects associated with metformin use are gastrointestinal and include bloating, flatus, and diarrhea. It is recommended that metformin be taken with food and initially administered at a low dose and titrated up to minimize these adverse effects. The most severe and life-threatening adverse effect associated with metformin is lactic acidosis. Prevention and early diagnosis and intervention of this condition is essential as it carries a mortality rate of up to 50% (34). While lactic acidosis was most frequently associated with the older

generation of biguanides (phenformin and buformin) resulting in their removal from the market in the 1970s, this warning has remained for metformin. Fortunately, this complication is rare with an incidence estimated at 3.3 cases per 100,000 patient-years of treatment (44). Interestingly, to put this into perspective, the estimated incidence of lactic acidosis in sulfonylurea-users is 4.8 cases per 100,000 patient-years (44). However, despite this low risk, it is recommended that therapeutic serum concentration of metformin not exceed 2.5 mg/L and that metformin doses be adjusted for renal impairment (34).

1.6. Metformin and the Phosphatidylinositol 3-Kinase (PI3K) Pathway

To better understand the role that metformin may play as an inhibitor of tumor cell proliferation, we must first understand the pathways involved in its mechanism of action. Disruption of the PI3K-AKT pathway is considered central to the role of metformin in both normal and neoplastic tissues. The PI3K pathway is a signal transduction pathway critical to a variety of cellular functions including cell proliferation and protein synthesis, cell survival, cell cycle progression, cellular metabolism, and angiogenesis. PI3Ks are a family of lipid kinases that function by phosphorylating the 3-hydroxyl group of phosphoinositides. There are three distinct classes of PI3Ks that are differentiated by their substrate specificity and regulation (45). Here we will focus on Class IA PI3Ks as these are the best described and most commonly implicated in human cancers (46).

Class IA PI3Ks are heterodimers consisting of a p110 catalytic subunit (of which there are three – p110α, p110β, and p110δ) and a p85 regulatory subunit. While both p110α and p110β are ubiquitously expressed and are involved in cellular

proliferation and insulin signaling, p110δ is primarily expressed on leukocytes and plays a role in immune function. At baseline, p85 binds to the N-terminus of the p110 subunit inhibiting its catalytic activity (47). Activation of Class IA PI3Ks can occur through one of several mechanisms. The typical initiating event in the activation is the binding of a growth factor ligand (e.g., epidermal growth factor (EGF), platelet-derived growth factor (PDGF), insulin-like growth factor-1 (IGF-1), insulin, etc.) to its receptor tyrosine kinase (RTK). This promotes dimerization of the receptor and autophosphorylation of tyrosine residues. Following this, p85 is recruited to the plasma membrane and binds either directly or indirectly, through adaptor proteins such as insulin receptor substrate-1 (IRS1) or GRB2-associated binder (GAB), with the RTK releasing its inhibition of the p110 catalytic subunit. PI3K can also be activated via Ras, which directly activates the p110 subunit independently of p85 (48). Of note, the PI3K pathway is one of the best characterized downstream effectors of Ras and plays an important role in Ras-mediated cell survival. The interplay between the Ras-Mitogen Activated Protein Kinase (Ras-MAPK) and PI3K pathways is reviewed in further detail below. Activation of PI3K generates phosphatidylinositol 3,4,5-triphosphate (PIP_3) from phosphatidylinositol 4,5-biphosphate (PIP_2), a process that is negatively regulated by the tumor suppressor phosphatase and tensin homolog (PTEN) through its lipid phosphatase activity, converting PIP_3 back to PIP_2. Loss of PTEN function, either by mutation or epigenetic silencing, results in uncontrolled PI3K activity which may ultimately lead to cancer. As we will see later, this is clinically important in endometrial cancer, which has a high frequency of cases with PTEN loss. PIP_3

recruits the serine-threonine kinase, AKT, to the plasma membrane. Docking of the pleckstrin homology (PH) domain of AKT to PIP_3 induces a conformational change in AKT exposing two amino-acid residues (T308 and S473) that must be phosphorylated for full activation of AKT. Phosphorylation of these residues is accomplished by 3-phosphoinositide-dependent protein kinase 1 (PDPK1) and the mTOR-rictor (rapamycin insensitive companion of mTOR) complex (mTORC2), respectively (49-51). Once AKT is fully activated it acts as a central node in the PI3K pathway, regulating a wide variety of cellular processes involved with cell survival, protein synthesis and proliferation, and cellular metabolism (52). One of the key downstream effectors by which AKT regulates protein synthesis is through the tuberous sclerosis 1/2 (TSC1/2) complex. AKT inactivates TSC1/2 which releases its inhibition on the mTOR-regulatory-associated protein of mTOR (Raptor) (mTORC1) complex. The mTORC1 complex propagates the growth signal by phosphorylating eukaryotic initiation factor 4E-binding protein (4E-BP) and p70 ribosomal S6 kinase (p70S6K) which promote ribosome biogenesis and protein synthesis. At baseline, this process is also regulated by another variable – the energy status of the cell. That is, at times of energy deprivation, there is an increase in the intracellular concentration of AMP relative to ATP. This increase in the ratio of AMP to ATP activates the cellular energy sensor AMPK. Activated AMPK, in an attempt to maintain cellular energy homeostasis, then phosphorylates TSC2 resulting in inhibition of mTORC1 signaling which down-regulates energy consuming processes such as protein synthesis. This is where metformin is believed to have its predominant direct effect on inhibition of cellular proliferation. As described above,

metformin inhibits mitochondrial respiratory chain complex I resulting in decreased ATP production, leading to an increase in the ratio of intracellular AMP to ATP, activation of AMPK, and ultimately to decreased mTORC1 signaling and decreased cellular proliferation.

1.7. Ras Activation and the MAPK Pathway

The Ras-MAPK and PI3K-AKT pathways are two of the best characterized intracellular signaling pathways. When first discovered, both of these pathways were thought to be linear pathways that existed in parallel and were even activated by different stimuli. However, as they have been further investigated and characterized, it is clear now that there is a high degree of cross-talk between both pathways. Ras has been shown to interact with the different isoforms of class IA PI3Ks (53-55). As such, to understand the role of Ras on PI3K signaling, we must first understand how Ras is regulated and activated. Ras proteins are GTPase binary molecular switches that regulate cell proliferation, differentiation, and survival. Four distinct Ras isoforms exist – H-Ras, N-Ras, K-Ras4A, and K-Ras4B - which exhibit a high degree of sequence homology in approximately the first 169 amino acids (56). The final 23-24 amino acids comprise what is termed the hypervariable region (HVR) that defines the isoform and contains the membrane interacting and targeting sequences (56). All Ras isoforms contain a carboxy terminal –CAAX motif, where C represents cysteine, A is usually an aliphatic amino acid, and X is any amino acid. This –CAAX motif directs a series of post-translational modifications that are necessary for activation and trafficking of the Ras protein to the inner leaflet of the plasma membrane which is required for signaling.

Newly synthesized Ras proteins immediately undergo a series of post-translational modifications, some of which are constitutive and irreversible and others that are conditional and reversible (57). First, -CAAX is constitutively processed and modified by three enzymes that appear to work in series resulting in polyisoprenylation, endoproteolysis, and carboxyl methylation (58). The end result is that the otherwise hydrophilic Ras proteins become hydrophobic at their C termini allowing them to associate with intracellular membranes. Indeed, endoproteolysis and carboxyl methylation are both accomplished on the cytoplasmic surface of the endoplasmic reticulum and Golgi apparatus (58). Once there, a "second signal" is required for trafficking of Ras proteins to the plasma membrane from endomembranes (56, 59). In the case of H-Ras, N-Ras, and K-Ras4A, palmitoylation of the HVR facilitates this translocation (60, 61). This process is dynamic in which depalmitoylation of H-Ras, N-Ras, and K-Ras4A mediates retrograde transport to the Golgi (62). For K-Ras4B (which will be referred to as simply K-Ras), the "second signal" has not yet been clearly defined, but is believed to involve diffusion down an electrostatic gradient involving the polybasic domain of the HVR (57, 59). That is, the net negative charge of the plasma membrane attracts the positively-charged polybasic domain of K-Ras. While K-Ras is predominantly distributed at the plasma membrane, studies have demonstrated that its association with the plasma membrane is also reversible and dynamic (63).

At the plasma membrane, in the basal state, GDP-bound Ras is inactive. Upon binding of growth factor ligands to their RTKs, guanine nucleotide exchange factors (GEFs), such as Son of Sevenless (SOS), are recruited to the plasma membrane by

GRB2 which activate Ras by promoting the release of GDP and allowing GTP binding. Activated Ras can then interact with Ras-binding domains (RBDs) on effector molecules, including PI3K among others. As is apparent, this process is similar to, and indeed involves the same growth factors as, that involved in activation of PI3K. The principal effector pathway of Ras is the MAPK pathway. This kinase cascade consists of a GTPase-regulated Ras that phosphorylates and activates RAF kinase which, in turn, phosphorylates and activates MEK which then phosphorylates and activates the effector kinase, extracellular-signal-related kinase-1/2 (ERK1/2). ERK1/2 is involved in promoting cell survival and proliferation and cell motility (52). However, constitutive activation of Ras as a result of oncogenic mutations may also lead to uncontrolled activation of the PI3K pathway which results in persistent pro-proliferative and pro-survival signaling regardless of the presence of growth factors. Ras activation is negatively regulated by GTPase-activating proteins (GAPs) which catalyze GTP hydrolysis to return Ras to the GDP-bound inactive state (57). Loss of GAPs is another mechanism by which Ras proteins may be constitutively activated. In the next section we will review the importance of RAS-PI3K interactions as it pertains to oncogenic signaling.

1.8. The Interaction Between Ras and PI3K in Tumorigenesis

Several authors have commented and provided preclinical evidence demonstrating the importance of PI3K in Ras-dependent oncogenic transformation (64-66). An overview of the key players in these pathways is demonstrated in Figure 1.

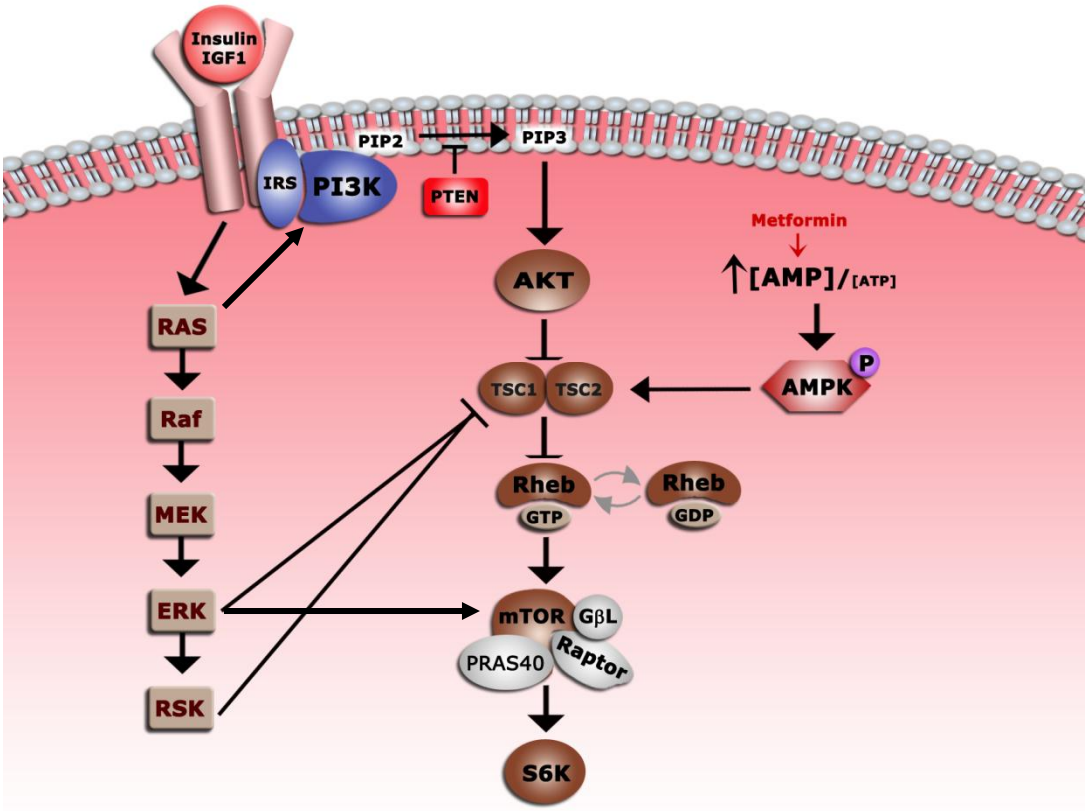

Figure 1. Overview of the PI3K and Ras-MAPK Pathways

It is also well accepted that Ras plays a critical role in both tumor initiation and maintenance. However, given the presence of multiple Ras effector pathways, it is important to identify what role each plays in Ras-dependent tumorigenesis. What is now known is that multiple effector pathways (MAPK, PI3K, and RalGEF) play critical roles in Ras-dependent tumor initiation. However, as tumorigenesis progresses, maintenance of Ras-dependent tumor growth seems to specifically require PI3K pathway activation (67). Both pathways appear to be highly integrated with mechanisms of cross-talk including cross-inhibition and cross-activation (52). The Ras-MAPK and PI3K-AKT pathways can negatively regulate each other. As a result, inhibition of one pathway may lead to activation of the other such as seen

with MEK inhibitors and AKT activation (68, 69). Cross-activation can also occur at several points. As described above, Ras-GTP can directly bind and allosterically activate PI3K. ERK1/2 which is downstream on the Ras-MAPK pathway can activate mTORC1 both indirectly by inhibiting TSC2 (70) at sites different than AKT which releases its inhibition and promotes mTORC1 activation and directly by phosphorylating Raptor (71). The clinical importance of this extensive cross-talk, particularly in endometrial cancer where these pathways are both frequently mutated, is the obvious need to target more than one pathway to inhibit cancer cell proliferation and tumor growth. Indeed, this need for dual pathway inhibition has been demonstrated by human cancer cells carrying alterations in the PI3K pathway which were responsive to the mTORC1 inhibitor RAD001, except when K-Ras mutations occurred concomitantly (72). Furthermore, in this same study, in a cohort of metastatic cancer patients, the presence of oncogenic K-Ras mutations was associated with lack of benefit after RAD001 therapy (72). Several authors have demonstrated that inhibition of both PI3K and Ras-MAPK pathways results in inhibition of tumor growth in prostate and lung cancer mouse models (73, 74) and of cellular proliferation in human cancer cell lines (75). However, these combination strategies may be limited in human studies secondary to dose-limiting toxicities. Thus, it is important to evaluate the role of more tolerable agents, such as metformin, as a potential component of a targeted combination therapeutic strategy. This is particularly important in endometrial cancer where both of these tumorigenic pathways are commonly aberrant.

1.9. Endometrial Cancer and Metformin

The importance of identifying novel therapeutic strategies for endometrial cancer is warranted due to its stable, if not increasing, incidence as a result of the growing worldwide obesity pandemic and associated medical comorbidities, which increase a woman's risk of developing the disease. Endometrial cancer is currently the most common gynecologic malignancy in the United States with an estimated 46,470 women diagnosed with uterine cancer and 8,120 estimated to have died of the disease in 2011 (76). Based on epidemiological and molecular factors, endometrial cancer can be subdivided broadly into two types which have important implications on prognosis and treatment options. Type I endometrial cancers account for approximately 80% of cases, are classically of endometrioid histology, and are associated with obesity and prolonged estrogen stimulation. Type II carcinomas are often of non-endometrioid histology, typically arise in a background of atrophic endometrium, and appear to be unrelated to estrogen stimulation. Obesity is an important risk factor for the development of endometrial cancer. The relative risk of uterine cancer-related death for women considered obese is 2.53, while for morbidly obese women it is 6.25 (77). Furthermore, the association between obesity and other medical co-morbidities, such as diabetes mellitus and insulin resistance, also contributes to mortality. The prevalence of diabetes in the general population is approximately 7% to 8% and continues to rise (78).

Type I and Type II ECs frequently demonstrate distinct molecular alterations that may serve to guide therapeutic treatment strategies. A summary of common genetic

alterations associated with Type I and Type II endometrial carcinomas is found in Table 1.

Genetic Alteration	Type I lesions (%)	Type II lesions (%)	References
PTEN loss of function	83	10	(79, 84)
PIK3CA mutation	36	5	(81, 86, 87)
Microsatellite Instability	20-30	0-11	(82, 87-89)
K-Ras mutation	15-26	0-5	(83, 84, 90)
β-catenin mutation	25-38	3	(86, 91)
p53 loss of function	10-17	93	(84, 92)
HER-2/neu overexpression	10	43	(87, 93)
p16 inactivation	10	45	(87, 92)

Table 1. Genetic alterations associated with Type I and Type II endometrial carcinomas

The most common genetic alteration associated with Type I lesions is a loss of function of PTEN which can be encountered in up to 83% of cases and 55% of precancerous lesions (79). Mutations in PTEN have been documented in endometrial hyperplasia and, thus, have been suspected to be an early event in the endometrial tumorigenesis process (80). As described above, PTEN plays a role in the regulation of the PI3K-AKT pathway by inhibiting the downstream phosphorylation of AKT, but its loss of function has also has been shown to result in genomic instability by causing defects in either homologous recombination DNA

repair or in cell cycle checkpoints. Mutations on PIK3CA, the gene coding for the catalytic subunit of PI3K, are seen in up to 36% of endometrioid cancers (81) and are often found in combination with PTEN mutations.

Other common genetic alterations associated with type I endometrial carcinomas include: microsatellite instability (MSI) and mutations in K-Ras. Approximately 20% to 30% of type I lesions exhibit MSI (82). Activating mutations in K-ras are observed in 15-26% of endometrioid carcinomas (83, 84). Although, Ras and PI3K pathway mutations are found to be mutually exclusive in other cancer types, in endometrial cancer, tumors with mutations in both pathways often coexist (48). In fact, up to 80% of tumors with a PIK3CA mutation also harbor a K-Ras and/or PTEN mutation (85). In contrast to Type I lesions, the genetic alteration most commonly seen in type II lesions is a p53 mutation, which is found in up to 90% of serous carcinomas (compared with 10% of type I lesions), and PTEN mutations are less common (84). The frequency of potentially targetable genetic alterations associated with endometrial carcinomas has resulted in considerable interest in novel therapeutic strategies for this malignancy.

As described above, metformin is one of the most commonly used hypoglycemic agents in the management of type II diabetes mellitus, which is associated with insulin resistance and an increased risk for the development of endometrial cancer. Several epidemiological studies have demonstrated that diabetic patients being treated with metformin have a reduced cancer incidence or improved response to chemotherapy when compared to diabetic patients receiving other oral hypoglycemic agents or insulin (78, 94, 95). DeCensi and colleagues completed a meta-analysis

of five observational studies of all cancer types and found that metformin was associated with a 31% decrease in CA risk (SRR 0.69, 95%CI 0.61-0.79) (95). In a study of 2,529 patients who received neoadjuvant chemotherapy for early-stage breast cancer, Jiralerspong and colleagues, reported that the rate of pathologic complete responses was 24% among diabetic patients using metformin compared with 8% for diabetic patients not using metformin ($p<0.007$) (78). While the effects of metformin on hepatocytes, skeletal muscle, and adipocyte metabolism are understood, the mechanisms by which metformin exerts these antineoplastic effects, have not yet been fully characterized.

Given the prevalence of PI3K-AKT pathway alterations associated with endometrial cancer and its frequent association with obesity and diabetes mellitus, this is a logical site in which to evaluate the role of metformin as a cancer therapeutic. However, to date, published reports on the effects of metformin on endometrial cancer are limited. In a study evaluating the pre-clinical effects of metformin, Cantrell and colleagues, using two endometrial cancer cell lines, demonstrated that metformin was a potent inhibitor of endometrial cancer cell proliferation that was partially mediated by activation of AMPK with a subsequent decrease in mTOR signaling (27). Furthermore, the addition of metform to paclitaxel demonstrated significant synergistic anti-proliferative effects through modulation of the mTOR signaling pathway (96). However, all cell lines used in both of these studies expressed functional PTEN. Because metformin is postulated to mediate its anti-neoplastic effects through activation of AMPK in opposition to PI3K hyperactivation and given the frequency with which PTEN loss occurs in endometrial

cancer, our objective was to evaluate and compare the effect of metformin on PTEN deficient versus PTEN wild-type endometrial cancer *in vitro* and *in vivo*.

In addition to alterations in PTEN, K-ras mutations represent another common genetic defect found in endometrial cancers. Activating mutations in K-ras have been shown in a mouse model to synergize with PTEN inactivation to accelerate tumorigenesis in both endometrial (97) and lung cancer (98). In light of the growing interest in personalized cancer therapy using biologic agents to target specific molecular pathways, we further sought to characterize the effects of metformin on endometrial tumors in which K-Ras is activated, either in isolation or accompanied by loss of PTEN.

The identification of differential responses to metformin based on the genetic fingerprint of individual endometrial tumors may have important implications in defining a subset of patients that will benefit from metformin therapy either alone or in combination with other targeted agents. Furthermore, an understanding of the molecular mechanisms underlying metformin's antiproliferative effect should lead to the development of novel combination therapies for the more effective treatment of a variety of cancers

2. Methods

2.1. Cell Culture

Hec1A, a well-differentiated human endometrial carcinoma cell line that expresses PTEN and harbors an activating K-Ras mutation were purchased from the American Type Culture Collection (ATCC, Manassas, VA). Hec1A cells were cultured in McCoy's 5A Modified Medium supplemented with 10% fetal bovine serum

(FBS), 10,000 U/mL penicillin and 10,000 mcg/mL streptomycin. Ishikawa, a well-differentiated human endometrial carcinoma cell line with loss of PTEN expression and wild-type K-Ras was purchased from the European Collection of Cell Cultures (ECACC, Porton Down, United Kingdom). Ishikawa cells were cultured in Dulbecco's Modified Eagle's Medium (DMEM) supplemented with 10% FBS, 2 mM L-glutamine, 1 mM sodium pyruvate, 0.1 M non-essential amino acids, 10,000 U/ml penicillin and 10,000 ug/ml streptomycin. MecPK, a mouse endometrial carcinoma cell line was derived and immortalized from the endometrial tumor of a transgenic mouse with homozygous PTEN deletion and a K-Ras mutation (*PTEN*$^{-/-}$*K-Ras*^{G12D}) (97) and was cultured in RPMI 1640 supplemented with 10% FBS and 10,000 U/mL penicillin and 10,000 ug/mL streptomycin. Cells were incubated at 37^{o}C under 5% CO_2 to 70% confluence before treatment.

2.2. Reagents and Inhibitors

Metformin (1,1-Dimethylbiguanide hydrochloride) was purchased from Sigma (St. Louis, MO) and dissolved in sterile PBS. BEZ235 (a dual inhibitor of pan-PI3K and mTOR) and RAD001 (an inhibitor of mTORC1) were purchased from Selleck Chemicals (Houston, TX) and dissolved in sterile dimethyl sulfoxide (DMSO). AZD6244 (a MEK inhibitor) was graciously provided by the lab of Dr. Kwong K. Wong at the University of Texas, M.D. Anderson Cancer Center.

2.3. Metformin Treatment Cell Viability Assays

To evaluate the effect of metformin on endometrial cancer cells *in vitro*, cell viability assays were performed. For all cell viability assays, endometrial cancer cells were seeded in 96-well plates at a density of 4 x 10^3 cells/well and were

incubated at 37^{o}C under 5% CO_2 for 24 hours prior to drug treatment. The medium was then replaced with fresh antibiotic-free medium containing metformin at concentrations ranging from 0.5 – 20 mM. After treatment for 48 hours, cells were incubated for 3.5 hours with MTT (3-(5-dimethylthiazol-2-yl)-2,5-diphenyltetrazolium bromide) dye at 37^{o}C under 5% CO_2. Following the incubation, the MTT reaction was halted with the addition of solvent containing 2-propanol, 0.1% NP40, and 4 mM HCL. Following the addition of MTT solvent, 96-well plates were shaken gently in the dark for 15 minutes. The absorbance of the purple formazan product catalyzed by metabolically active cells was recorded at a wavelength of 590nm with 620nm as a background. The change in the optical density (ΔOD) measured at these two wavelengths was calculated. Data are expressed as the relative absorbance normalized to control PBS-treated cells. Three independent assays were performed in triplicate.

2.4. Western Blot Analysis Following Metformin Treatment

To evaluate the effect of metformin on protein expression and downstream signaling in the PI3K and Ras-MAPK pathways, endometrial cancer cells were seeded on 6-well plates at a density of 2 x 10^5 cells/well and were incubated at 37^{o}C under 5% CO_2 for 24 hours prior to metformin treatment. The medium was then replaced with fresh antibiotic-free medium containing metformin at concentrations of 1 mM, 5 mM, and 10 mM for 48 hours. At 48 hours of treatment, the media was discarded and whole cell lysates were collected with Mammalian Protein Extraction Reagent (M-PER) (ThermoScientific, Rockford, IL) containing phosphatase inhibitor (1:100) and protease inhibitor (1:10).

Protein extraction was accomplished by first discarding the media from each well. Wells were then washed with sterile PBS. Immediately afterwards, 100 uL of M-PER, containing protease and phosphatase inhibitors, was added to each well and incubated on ice at 4^0C for 30 minutes. Cells were then mechanically lysed with a spatula and collected into separate, ice-cold 1.5 mL centrifuge tubes. Tubes were centrifuged at 13,000 rpm for 15 minutes at 4^0C. Following centrifugation, the supernatant from each tube was collected and transferred into new, ice-cold 1.5 mL centrifuge tubes and the cell pellets were discarded. To calculate the protein concentration, Bio-Rad Protein Assay Dye Reagent Concentrate (Bio-Rad Laboratories, Hercules, CA) was mixed with ddH_20 at a ratio of 1:4 (total volume depending on the number of samples). A total of 2 uL of protein sample was added to 1 mL of dilute protein assay dye into separate cuvettes. Samples were vortexed thoroughly and allowed to sit at room temperature for 5 minutes before measuring the absorbance of each sample at 595nm using Bio-Rad SmartSpec^{TM} 3000 (Bio-Rad Laboratories, Hercules, CA). Concentrations were calculated using the Bradford formula.

Equal amounts of protein (15 ug) were separated by sodium dodecyl sulfate-polyacrylamide gel electrophoresis (SDS-PAGE) using a 10% gel at 110V. Proteins were then transferred onto a nitrocellulose membrane using a current of 0.2 amps over 2.5 hours. Membranes were washed briefly with non-sterile 1X PBS with 20% Tween-20 (1X PBST) and blocked with 5% nonfat dry milk for 30 minutes and incubated overnight with gentle shaking at 4^0C using a 1:1000-2000 dilution of the primary antibody of interest in 5% nonfat dry milk. Primary antibodies directed

against phospho-AMPKα (Thr172), Total AMPK, phospho-Akt (Ser473), Total Akt, phospho-p44/42 MAPK (Erk1/2) (Thr202/Tyr204), and phospho-S6 ribosomal protein (Ser235/236) were used. All antibodies were purchased from Cell Signaling (Beverly, MA) unless otherwise indicated. As a loading control, β-actin expression was detected using anti-β-actin IgG (Sigma, St. Louis, MO). Following overnight incubation with primary antibody, membranes were washed thrice for 10 minutes each using non-sterile 1X PBST and then incubated with a secondary anti-mouse or anti-rabbit horseradish peroxidase-conjugated antibody (GE Healthcare UK Limited, Buckinghamshire, United Kingdom) for 1 hour. Secondary antibody was prepared by adding 3 uL of either anti-mouse or anti-rabbit horseradish peroxidase-conjugated antibody to 5 mL of ddH_20 mixed with an additional 5mL of 5% nonfat dry milk. Membranes were then washed four times for 15 minutes each in 1X PBST. Antibody binding was enhanced using SuperSignal® West Dura Extended Duration Substrate (ThermoScientific, Rockford, IL) and developed. In a similar fashion, the PTEN and OCT1 expression status for each cell line was determined by western immunoblotting using primary antibodies directed against PTEN (Cell Signaling, Beverly, MA) and SLC22A1 (Sigma, St. Louis, MO), respectively.

2.5. Cell Cycle Analysis Following Metformin Treatment

To evaluate the effect of metformin on the cell cycle and apoptosis in endometrial cancer cells, flow cytometric analysis was performed. Endometrial cancer cells were seeded on 6-well plates at a density of 2 x 10^5 cells/well and were incubated at 37^{o}C under 5% CO_2 for 24 hours prior to metformin treatment. The cells were then treated with fresh antibiotic-free medium containing metformin at

concentrations of 1 mM, 5 mM, 10 mM, and 20 mM for 48 hours. After 48 hours, cells were trypsinized, transferred to separate 15 mL sterile culture tubes, washed in 1X PBS, and centrifuged at 1,500 rpm for 5 minutes. Cells were then resuspended and fixed in 70% ethanol for a minimum of 24 hours at 4^0C with gentle shaking. Cells were then centrifuged at 2,500 rpm for 5 min, washed with 1X PBS, and resuspended in staining solution containing: 40 µg/mL propidium iodide, 80 µg/mL RNase A in PBS supplemented with 0.1% Triton X-100 and 0.1 mM EDTA. Cells were incubated in the staining solution at room temperature for 30 minutes before cell cycle analysis was performed using the Gallios Flow Cytometer (Beckman Coulter, Indianapolis, IN) according to the manufacturer's protocol. Kaluza Flow Cytometry Analysis v1.1 software (Beckman Coulter) was used to calculate the cell cycle distribution from the histogram. Apoptotic cells were determined on the histogram as the percentage of cells in the sub-G1 peak.

2.6. In Vivo Xenograft Study

To validate our *in vitro* results in a xenograft mouse model, 60 female athymic nude mice were purchased from the National Institutes of Health (Bethesda, MD) and housed at 5 mice per cage in a specific pathogen-free facility. Nude mice were maintained in accordance with guidelines established by the Institutional Animal Care and Use Committee. At 6-weeks of age, intraperitoneal injections were performed on each mouse in the midline lower abdomen with 5×10^6 early-passage endometrial cancer cells (20 injected with Hec1A cells, 20 injected with Ishikawa cells, 20 injected with MecPK cells). Tumors were allowed to progress for 7 days prior to initiating either control or metformin treatment. Each group of 20 mice per

cell line was divided into two subgroups of 10 mice each. Ten mice were treated with metformin dissolved in drinking water (5 mg/mL) and the remaining ten mice were provided untreated sterile drinking water. Both metformin-treated water and control untreated water were changed twice weekly on Tuesdays and Fridays. Treatment continued until at least one mouse became moribund, at which time all animals in the same endometrial cancer cell line group were euthanized. Serum was collected immediately and was stored at -80^{o}C. Serum from each mouse was sent for analysis of liver chemistries. Mice were weighed prior to necropsy and all visible tumor was carefully dissected from all peritoneal surfaces. Tumors were then weighed, a representative portion of tumor was fixed in formalin, and the remainder was flash frozen and stored at -80^{o}C.

2.7. Immunohistochemical Analysis of Xenograft Tumor Tissues

Slides were cut from formalin-fixed, paraffin-embedded tissue blocks for both Hec1A and Ishikawa and were then used for immunohistochemical analysis of tumor phosphorylated S6 ribosomal protein (pS6rp) expression as a downstream marker of PI3K/AKT pathway signaling and Ki-67 staining as a marker for proliferation. Immunohistochemistry staining was carried out by first baking slides in a 60^{0}C oven for 30 minutes. Slides were then deparaffinized by washing in xylene thrice for 10 minutes each. Slides were then rehydrated in serial graded ethanol – 100%, 100%, 100%, 80%, 80%, ddH_2O for 3 minutes each. Finally, slides were rinsed in 1X PBS for 5 minutes. Antigen retrieval was accomplished by first placing slides in a citrate buffer bath (pH 6.0) and bringing the bath to a slow boil. Slides in the citrate buffer bath were then transferred into a pressure cooker and the temperature increased to

120^0C. Slides were incubated in the pressure cooker at 120^0C for either 9 minutes (Ki-67) or 11 minutes (pS6rp). At the desired antigen retrieval time, the pressure cooker was turned off and slides were removed and allowed to cool at room temperature in the citrate buffer bath for 30-60 minutes. Following antigen retrieval, slides were submerged in 3% H_2O_2 for 10 minutes to block endogenous peroxidase activity. After blocking slides with 1% normal goat serum for 15 minutes, primary antibody was applied and slides were incubated overnight at 4^0C in a humidified chamber. The primary antibodies used were phosphorylated S6 ribosomal protein (S235/236) rabbit monoclonal antibody (Cell Signaling Technology, Beverly, MA) at 1:50 dilution and purified mouse anti-human Ki-67 monoclonal antibody (BD Biosciences, San Diego, CA) at 1:50 dilution. Following overnight incubation, slides were washed in 1X PBST twice for 5 minutes to remove the primary antibody. Slides were then treated with biotin-labeled affinity isolated goat anti-rabbit and goat anti-mouse immunoglobulins in PBS (DakoCytomation, Carpinteria, CA) for 10 minutes followed by a wash in PBS and then application of streptavidin-horseradish peroxidase solution (DakoCytomation, Carpinteria, CA) for 10 minutes. Slides were rinsed in PBS and developed with 3,3'-diaminobenzidine (DakoCytomation, Carpinteria, CA) for 1 minute and 45 seconds, rinsed in tap water, counterstained in 10% hematoxylin, and dehydrated in serial graded ethanol.

Phosphorylated S6rp expression was scored as the product of the percentage of cells staining positive (0 = <10%; 1 = 10-25%; 2 = 26-50%, 3 = 51-75%, and 4 = >75%) and the intensity of the staining (1 = weak; 2 = moderate; 3 = strong). For the proliferation index, the average of the ratio of positive Ki-67 stained nuclei to total

nuclei in $\geq$ 3 representative high-powered fields from each specimen was determined.

2.8. Transfection of MecPK Cells for Stable Expression of PTEN

To determine whether the expression of PTEN alters the proliferative or cell viability response to metformin treatment, MecPK cells were transfected to stably express PTEN. MecPK cells were seeded on 6-well plates at a density of 2 x 10^5 cells/well and were incubated at 37^oC under 5% CO_2 for 24 hours. For transfection, a pIRES2-EGFP plasmid (Clontech Laboratories, Mountain View, CA) was used to construct a vector with and without PTEN inserted that also contained a neomycin/kanamycin-resistance domain to allow for stable selection of PTEN expressing cells. A plasmid lacking a neomycin-resistance domain, pCMV5-FLAG-PTEN, from which we obtained the PTEN gene for our plasmid vector was graciously provided by the lab of Dr. Gordon Mills (University of Texas, M.D. Anderson Cancer Center).

DH5α competent bacteria were thawed on ice and transformed by incubating with the pIRES2-EGFP vector diluted 1:10 in sterile ddH_2O in vented conical tubes. During the transformation, bacteria were placed on ice for 30 minutes followed by a heat shock at 42^0C for 1 minute to promote plasmid uptake by bacteria. Bacteria were then placed on ice for an additional 2 minutes prior to adding 1 mL lysogeny broth (LB) to each tube. Bacteria were then incubated at 37^0C for one hour and then plated on LB Agar Kanamycin-50 100mm plates (Sigma, St. Louis, MO) and incubated overnight at 37^0C. Following overnight incubation, one colony was selected from the plate using a sterile toothpick and placed in a vented 15 mL

conical tube in 3 mL of LB and incubated at 37^0C for 16 hours with vigorous shaking. At the completion of the 16 hour incubation, 1 mL of the LB containing transformed bacteria was transferred into two separate 1.5 mL centrifuge tubes. Bacterial cells were harvested by centrifugation at 13,000 rpm for 3 minutes at room temperature. The supernatant was discarded and a QIAprep Spin Miniprep Kit (Qiagen Sciences, Venlo, Netherlands) was used to purify plasmid DNA per the manufacturer's instructions. The restriction map of pCMV5-FLAG-PTEN demonstrated that the PTEN gene is flanked by restriction sites for EcoRI and BamHI restriction enzymes (Promega, Madison, WI). The restriction map of pIRES2-EGFP also demonstrated that the multiple cloning site contains restriction sites for both EcoRI and BamH1. Both pIRES2-EGFP and pCMV5-FLAG-PTEN plasmids were independently digested using a mixture of 10 uL of plasmid DNA, 2 uL 10X E Buffer (Promega, Madison, WI), 1 uL BamHI, 1 uL EcoRI, and 6 uL of ddH_2O and incubated at 37^0C for 1 hour. During the last 15 minutes of the digestion for pIRES2-EGFP, 1 uL of shrimp alkaline phosphatase was added to the mixture to remove the phosphates and prevent re-annealing. DNA fragments were separated on a 1% agarose gel at 80V for 1 hour. The bands corresponding to PTEN (1.3kb) and linearized pIRES2-EGFP (5kb) were cut out and extracted from the gel using the QIAEX II Agarose Gel Extraction Kit (Qiagen Sciences, Venlo, Netherlands) per the manufacturer's instructions. Ligation of the PTEN gene insert into the linearized pIRES2-EGFP vector was accomplished using a mixture of 4 uL 5X ligase, 4 uL linearized pIRES2-EGFP DNA, 4 uL PTEN gene insert DNA, 1 uL T_4 ligase, and 7 uL of ddH_2O. Following ligation, DH5α competent bacteria were transformed, using methods

previously described above, with either pIRES2-EGFP-PTEN, linearized pIRES2-EGFP, and ligated pIRES2-EGFP and cultured on LB Agar Kanamycin-50 100mm plates (Sigma, St. Louis, MO) and incubated overnight at 37^0C. Colonies were selected from plates containing bacteria transformed with pIRES2-EGFP-PTEN and ligated pIRES2-EGFP and transferred to vented conical tubes containing LB with a 1:1000 dilution of kanamycin and incubated at 37^0C for 16 hours. As expected, plates seeded with bacteria transformed with linearized pIRES2-EGFP did not develop colonies resistant to kanamycin. Plasmid DNA purification using the QIAprep Spin Miniprep Kit was performed as described above followed by digestion of plasmid DNA using BamHI and EcoRI restriction enzymes and separation of DNA fragments on a 1% agarose gel to confirm insertion of PTEN in the pIRES2-EGFP-PTEN plasmids and absence of PTEN in the pIRES2-EGFP control plasmids.

For transfection, 4 ug of plasmid DNA was used per well of a 6-well plate and performed using Lipofectamine 2000 (Invitrogen, Carlsbad, CA). One day before transfection, 2×10^5 MecPK cells were plated per well in 2 mL of antibiotic-free RPMI 1640 growth medium supplemented with 10% FBS and incubated at 37^0C overnight to reach 80-90% confluence at the time of transfection. One well was transfected with pIRES2-PTEN, one well with pIRES2 vector alone (as a negative control), one well with Lipofectamine 2000 alone (mock transfection), and three untransfected wells without Lipofectamine 2000. Media containing Lipofectamine 2000 was replaced after 6 hours with fresh media. After 24 hours, G418-sulfate 750 ug/mL (Cellgro, Manassas, VA) was applied to the two transfected wells and the mock transfected well. Concurrently, a titration experiment using G418-sulfate on

untransfected MecPK cells found that a concentration of 500 ug/mL to 750 ug/mL was sufficient to kill all cells within 5-7 days. In transfected wells, media with G418-sulfate was replaced every 3 days until resistant colonies were identified. Five resistant colonies from each well were selected and expanded. Whole cell lysates were collected as per the protocol described above and were analyzed for PTEN expression by western blot analysis. To verify PTEN functionality, expression of pS6rp, as a downstream read-out of the PI3K pathway, was evaluated.

MecPK cells stably expressing PTEN and negative controls transfected with pIRES2-EGFP vector alone were seeded in 96-well plates at a density of 4 x 10^3 cells/well and were incubated at 37^{o}C under 5% CO_2 for 24 hours. The medium was then replaced with fresh antibiotic-free medium containing metformin at concentrations ranging from 0.5 – 20 mM. After treatment for 48 hours, MTT assays were performed as described above to compare differences in relative cell viability between MecPK cells expressing PTEN and those with loss of PTEN. Three independent assays were performed in triplicate.

2.9. Transient Silencing of K-Ras with siRNA

To determine whether inhibition of mutant K-Ras signaling reduced the inhibitory effects of metformin on cell proliferation and viability, K-Ras expression was transiently silenced in MecPK cells using siRNA. MecPK cells were seeded on 96-well plates at a density of 4 x 10^3 cells/well and were incubated at 37^{o}C under 5% CO_2 for 24 hours. Equal numbers of wells were transfected with either siGENOME SMARTpool K-Ras siRNA (Dharmacon, Lafayette, CO) or siGENOME non–targeting siRNA (Dharmacon, Lafayette, CO) using RNAiMax (Invitrogen, Carlsbad, CA) as

per the manufacturer's protocol. Media was replaced after 6 hours with fresh media containing increasing concentrations of metformin (0.5 – 20 mM). After treatment for 48 hours, MTT assays were performed as described above to compare differences in relative cell viability between MecPK cells expressing mutant K-Ras and those with silenced K-Ras. Three independent assays were performed in triplicate.

2.10. Transfection of Ishikawa Cells for Stable Expression of Oncogenic K-RasG12D Mutant

To determine whether expression of mutant K-Ras increased the susceptibility of a cell to metformin treatment compared to wild-type K-Ras, Ishikawa cells were transfected to stably express an oncogenic K-RasG12D mutant. Ishikawa cells were seeded on 6-well plates at a density of 2×10^5 cells/well and were incubated at 37^oC under 5% CO_2 for 24 hours. For transfection, a pMEV-2HA plasmid vector (Biomyx Technology, San Diego, CA) was used with and without oncogenic K-RasG12D inserted. Plasmids were graciously provided by the lab of Dr. Kwong K. Wong at the University of Texas, M.D. Anderson Cancer Center. For plasmid DNA transfection, 4 ug of plasmid DNA was used per well of a 6-well plate and performed using Lipofectamine 2000 (Invitrogen, Carlsbad, CA) as per the manufacturer's protocol. One well was transfected with pMEV-KRAS-G12D, one well with pMEV vector alone (as a negative control), and one well with Lipofectamine 2000 alone (mock transfection). Media containing Lipofectamine 2000 was replaced after 6 hours with fresh media. After 24 hours, G418-sulfate 750 ug/mL was applied to transfected wells and replaced every 3 days until resistant colonies were identified. All Ishikawa cells in the mock transfection well were killed within 7 days with G418-sulfate 750

ug/mL. Five resistant colonies were selected from each well and expanded and ultimately analyzed for K-Ras expression at the mRNA level by quantitative RT-qPCR.

Cells were first trypsinized and transferred to fresh labeled 1.5 mL centrifuge tubes. Tubes were centrifuged at 500 x *g* for 10 minutes to pellet the cells and the supernatant was then discarded. Cell pellets were resuspended in 500 uL of Trizol reagent (Life Technologies, Carlsbad, CA) followed by the addition of chloroform at a dilution of 1:5. Samples were vortexed and incubated at room temperature for 15 minutes. Samples were then centrifuged at 13,000 rpm for 15 minutes at 4^0C. The upper, aqueous phase containing the RNA was transferred to fresh, ice-cold 1.5 mL centrifuge tubes. RNA was precipitated by adding 500 uL of 2-propanol to each sample and incubating overnight at -20^0C. Following the incubation, samples were centrifuged at 13,000 rpm for 15 minutes at 4^0C to pellet the RNA. RNA was then washed twice in 75% ethanol. Following centrifugation, the supernatant was discarded and the RNA pellets were allowed to air-dry at room temperature for 15 minutes. The RNA pellets were then resuspended in approximately 15-30 uL of DEPC/RNase-free water (Ambion, Carlsbad, CA). RNA concentrations were quantified using the Bio-Rad SmartSpec^{TM} 3000 (Bio-Rad Laboratories, Hercules, CA). Aliquots from each sample were then treated with DNaseI. RT-qPCR using primers for 18S (Applied Biosystems, Carlsbad, CA) and human KRAS (Applied Biosystems, Carlsbad, CA) was performed to determine mRNA expression of KRAS in selected clones. The PCR protocol utilized was as follows: 50^0C for 10 minutes

and 95^0C for 5 minutes, followed by 95^0C for 12 seconds and 60^0C for 30 seconds for 40 cycles.

The clone demonstrating the greatest expression of K-Ras relative to negative controls was selected for viability assays. Ishikawa cells expressing oncogenic K-RasG12D and their corresponding negative controls were seeded in 96-well plates at a density of 4 x 10^3 cells/well and were incubated at 37^oC under 5% CO_2 for 24 hours. The medium was then replaced with fresh antibiotic-free medium containing metformin at concentrations ranging from 0.5 – 20 mM. After treatment for 48 hours, MTT assays were performed as described above to compare differences in relative cell viability between Ishikawa cells expressing the oncogenic K-RasG12D mutant and those with wild-type K-Ras expression. Three independent assays were performed in triplicate.

2.11. Confocal Imaging Analysis of the Effect of Metformin Treatment on Subcellular K-Ras Localization

As Ras transport to the plasma membrane is critical to its activation and intracellular signaling, a series of experiments were performed to evaluate the effect of metformin on Ras localization. Specifically, K-Ras and H-Ras localization was analyzed by confocal microscopy using Madin-Darby Canine Kidney (MDCK) cells expressing GFP-labeled oncogenic K-RasG12V or H-RasG12V mutants. These experiments were performed in collaboration with the lab of Dr. John Hancock at the University of Texas – Houston Medical School. MDCK cells were cultured in DMEM (ThermoScientific, Waltham, MA) supplemented with 10% FBS and 1 mM sodium pyruvate and plated at a density of 1 x 10^5 cells/well on coverslips in 12-well plates

and incubated at 37^0C, 5% CO_2 overnight. Cells were treated with vehicle (PBS) or metformin (0.001 – 2 mM) for 48 hours to allow new protein synthesis and trafficking. After treatment, cells were fixed with 4% paraformaldehyde at room temperature for 30 minutes and quenched with 50mM ammonium chloride for 10 minutes. Coverslips were mounted onto slides in Mowiol and imaged by confocal microscopy using a Nikon A1R Confocal Laser Microscope (Nikon, Tokyo, Japan). Three independent experiments were performed in which three representative fields from each slide were imaged and analyzed using ImageJ software. The ratios of membrane-bound GFP-labeled K-Ras and H-Ras to total (membrane + cytoplasmic) K-Ras and H-Ras were calculated. A similar experiment was performed in Hec1A cells transfected with GFP-labeled K-RasG12V and treated with 0.1 to 5 mM of metformin over 48 hours.

2.12. Analysis of the Effect of Metformin Treatment on Subcellular K-Ras Localization in a Human Endometrial Cancer Cell Line

To confirm and validate the results obtained using confocal microscopy on human endometrial cancer; subcellular fractionation was carried out in Hec1A cells to quantify the proportion of membrane-bound K-Ras compared to total K-Ras as a function of metformin treatment. Hec1A cells were plated at a density of 2 x 10^6 cells per plate on 100mm plates and incubated overnight in antibiotic-free medium at 37^oC, 5% CO_2. Cells were then treated with vehicle (1X PBS) or metformin (0.1 mM, 0.5 mM, 1 mM, and 5 mM) for 48 hrs. Following treatment, cell fractionation was performed using a Subcellular Protein Fractionation Kit (ThermoScientific, Waltham, MA) as per the manufacturer's protocol to extract the membrane and cytoplasmic

fractions. Cells were harvested with trypsin-EDTA and separated by treatment into in different 15 mL conical tubes. Cells were centrifuged at 500 x *g* for 5 minutes and the media supernatant was discarded. The cell pellet was resuspended in ice-cold 1X PBS. Cells were counted and a total of 6 x 10^6 cells from each treatment group were transferred into separate pre-chilled 1.5 mL centrifuge tubes. Cells were centrifuged at 500 x *g* for 3 minutes. The supernatants were discarded and the cell pellets were resuspended in 350 uL of cytoplasmic extraction buffer (CEB) containing a 1:100 dilution of Halt^{TM} Protease Inhibitor Cocktail (ThermoScientific, Waltham, MA). After adding the CEB to the cell pellet, cells were incubated at 4^0C for 10 minutes with gentle mixing. Following the incubation, cells were centrifuged at 500 x *g* for 5 minutes. The supernatant, representing the cytoplasmic protein fraction, was immediately transferred to separate pre-chilled 1.5 mL centrifuge tubes and labeled. The cell pellet was then resuspended in 350 uL of membrane extraction buffer (MEB) containing a containing a 1:100 dilution of protease inhibitor, vortexed vigorously for 5 seconds, and then incubated at 4^0C for 10 minutes with gentle mixing. Following the incubation, cells were centrifuged at 3000 x *g* for 5 minutes. The supernatant, representing the membrane protein fraction, was immediately transferred to separate pre-chilled 1.5 mL centrifuge tubes and labeled. Protein concentrations from the membrane and cytoplasmic fractions were determined as described by the methods above and equal amounts of protein (15 ug) were separated by SDS-PAGE using a 12% gel and transferred onto a nitrocellulose membrane. Membrane and cytoplasmic fractions were run on the same gel. Rabbit monoclonal Na+/K+ ATPase alpha antibody (Epitomics,

Burlingame, CA) and total AKT (Cell Signaling, Beverly, MA) were used as loading controls and to confirm the purity of membrane and cytoplasmic fractions, respectively. Primary monoclonal anti-c-K-Ras, clone 234-4.2 (Sigma, St. Louis, MO) was used to evaluate the expression of K-Ras in each cellular fraction. Densitometry analyses of western immunoblots were carried out using ImageJ software and the ratio of membrane-bound K-Ras to total (membrane + cytoplasmic) K-Ras was calculated. Three independent experiments were performed in triplicate.

2.13. Analysis of the Effect of Aminoimidazole-4-Carboxamide Riboside (AICAR) Treatment on Subcellular K-Ras Localization

AICAR (Cell Signaling, Beverly, MA) is an AMP analog that promotes activation of AMPK by increasing the ratio or intracellular AMP to ATP. As this is a mechanism by which metformin is thought to also exert its anti-proliferative effects, we sought to evaluate whether AMPK activation by AICAR would affect subcellular K-Ras localization. Hec1A cells were plated at a density of 2×10^6 cells per plate on 100mm plates and incubated overnight in antibiotic-free medium at 37^oC, 5% CO_2. Cells were then treated with either vehicle (1X PBS), metformin (1 mM and 5 mM), or AICAR (0.1 mM and 1 mM) for 48 hours. Following treatment, cell fractionation was performed in a similar manner as described above using a Subcellular Protein Fractionation Kit (ThermoScientific, Waltham, MA) to extract the membrane and cytoplasmic fractions. Equal amounts of protein (15 ug) were separated by SDS-PAGE using a 12% gel and transferred onto a nitrocellulose membrane. Membrane and cytoplasmic fractions were run on the same gels. Rabbit monoclonal Na+/K+ ATPase alpha antibody (Epitomics, Burlingame, CA) and total AKT (Cell Signaling,

Beverly, MA) were again used as loading controls. Primary monoclonal anti-c-K-Ras, clone 234-4.2 (Sigma, St. Louis, MO) was used to evaluate the expression of K-Ras in each cellular fraction. Densitometry analysis of western immunoblots was carried out using ImageJ software and the ratio of membrane-bound K-Ras to total (membrane + cytoplasmic) K-Ras was calculated. Two independent experiments were performed in triplicate.

2.14. Analysis of the Effect of Co-Treatment of Compound C, an AMPK Inhibitor, with Metformin or AICAR on Subcellular K-Ras Localization

To determine whether changes in subcellular K-Ras localization are AMPK-dependent, we sought to evaluate whether concurrent treatment with Compound C, an inhibitor of AMPK, would abrogate the effects seen with either metformin or AICAR. Hec1A cells were plated at a density of 2×10^6 cells per plate on 100mm plates and incubated overnight in antibiotic-free medium at 37^oC, 5% CO_2. Cells were then treated with either DMSO (control), metformin 5 mM +/- Compound C 10 uM, or AICAR 1 mM +/- Compound C 10 uM for 48 hours. Compound C was administered 1 hour prior to initiating treatment with either metformin or AICAR. Following 48 hours of treatment, cell fractionation was performed in a similar manner as described above using a Subcellular Protein Fractionation Kit (ThermoScientific, Waltham, MA) to extract the membrane and cytoplasmic fractions. Equal amounts of protein (15 ug) were separated by SDS-PAGE using a 12% gel and transferred onto a nitrocellulose membrane. Membrane and cytoplasmic fractions were run on the same gels. Rabbit monoclonal Na+/K+ ATPase alpha antibody (Epitomics, Burlingame, CA) and total AKT (Cell Signaling) were again used as loading controls.

Primary monoclonal anti-c-K-Ras, clone 234-4.2 (Sigma, St. Louis, MO) was used to evaluate the expression of K-Ras in each cellular fraction. Densitometry analyses of western immunoblots were carried out using ImageJ software and the ratio of membrane-bound K-Ras to total (membrane + cytoplasmic) K-Ras was calculated. Two independent experiments were performed in triplicate.

2.15. Combination of Metformin with PI3K inhibitors or MEK inhibitor

To evaluate the role of metformin in combination with other targeted agents, a series of MTT viability assays and western immunoblots were performed. MecPK cells were seeded on 96-well plates at a density of 4 x 10^3 cells/well and incubated at 37^{o}C under 5% CO_2 for 24 hours. Cells were treated with either DMSO (control), metformin alone (1, 5, and 10 mM), an mTOR inhibitor alone (RAD001 10 and 30 nM), a dual inhibitor of pan-PI3K and mTOR alone (BEZ235 100 and 500 nM), a MEK inhibitor alone (AZD6244 2 and 10 uM), or the combination of each targeted biologic agent with metformin. After 48 hours of treatment, MTT assays were performed as described above to compare differences in relative cell viability between each drug alone or different combinations at their approximate half maximal inhibitory concentration (IC50). Three independent experiments were performed in triplicate.

To evaluate the effect of combination therapies on the PI3K and Ras-MAPK signaling pathways, MecPK cells were seeded on 6-well plates at a density of 3 x 10^5 cells/well and were incubated at 37^{o}C under 5% CO_2 for 24 hours. Cells were then treated with either DMSO, metformin 5 mM alone, RAD001 10 nM alone, AZD6244 6 uM alone, or the combination of RAD001 10 nM plus metformin 5 mM or

RAD001 10 nM plus AZD6244 6 uM. Cells were treated for 48 hours after which whole cell lysates were harvested and total protein concentrations were calculated as described above. Equal amounts of protein (15 ug) were separated by SDS-PAGE using 10% gels and then transferred onto a nitrocellulose membranes. Membranes were incubated overnight at 4^0C with 1:1000 dilutions of primary antibodies directed against phospho-AMPKα (Thr172), Total AMPK, phospho-Akt (Ser473), Total Akt, phospho-p44/42 MAPK (Erk1/2) (Thr202/Tyr204), and phospho-S6 ribosomal protein (Ser235/236) - all purchased from Cell Signaling (Beverly, MA). β-actin expression served as a loading control and was detected using anti-β-actin IgG (Sigma, St. Louis, MO). Three independent experiments were performed. A similar experiment treating MecPK cells with either DMSO, BEZ235 250 nM alone, metformin 5 mM alone, metformin 10 mM, and the combination of BEZ235 250 nM with either metformin at 5 mM or 10 mM was also completed.

2.16. Statistical Analyses

The values obtained are presented as the mean $\pm$ SEM and analyzed using the Student's t-test or the Mann-Whitney U test (GraphPad Prism, version 5). Dose-response curves were converted into logarithmic curves and IC50 values calculated using GraphPad Prism, version 5 software. For all results, significance was set as $p < 0.05$. The data presented are the results of three independent experiments performed in triplicate unless otherwise indicated.

3. Results

3.1. Metformin Significantly Inhibits Proliferation of K-Ras Mutant Endometrial Cancer Cell Lines

To study the effects of metformin on endometrial cancer cell viability and proliferation, Hec1A, Ishikawa, and MecPK cells were treated with various concentrations (0.5–20 mM) of metformin over 48 hours. Metformin significantly inhibited the relative viability of MecPK and Hec1A cells in a concentration-dependent manner with a significant decrease in relative cell viability achieved at concentrations of 0.5 mM ($p=0.008$) and 5 mM ($p<0.001$), respectively. The mean IC50 was 1.16 mM for MecPK cells and 4.23 mM for Hec1A (Figure 2). In contrast, Ishikawa cell proliferation was significantly inhibited only at the highest metformin concentration (20 mM, $p=0.015$) and the IC50 could not be calculated based on the concentrations of metformin administered.

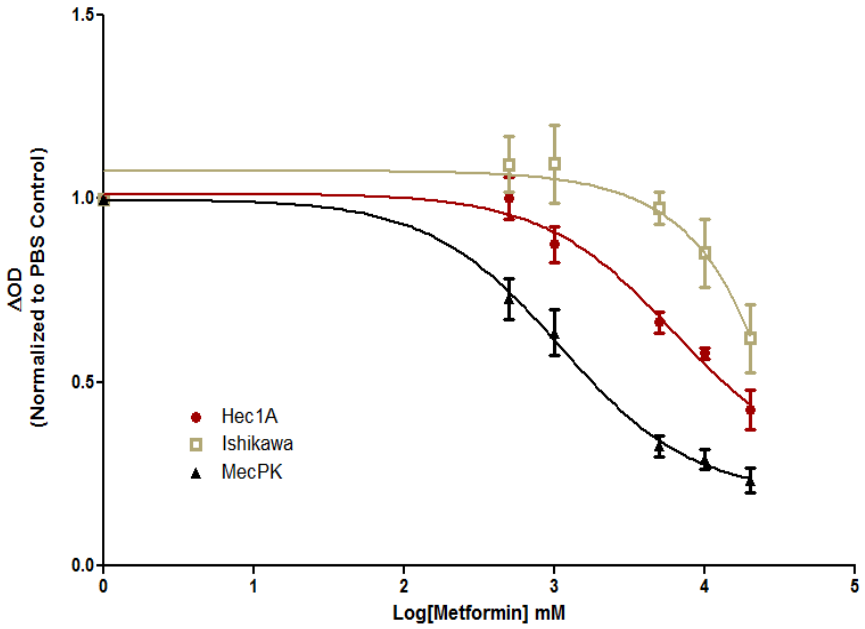

Figure 2. Log-scale dose-response curves for metformin treatment over 48h in Hec1A, Ishikawa, and MecPK cells. Metformin causes a significant concentration-dependent decrease in relative survival in both MecPK and Hec1A. In contrast, in Ishikawa cells, a significant decrease in relative cell viability was seen only at the highest concentration used (20mM). These data represent three independent experiments performed in triplicate. Error bars indicate +/- SEM.

3.2. Effect of Metformin on Expression of AMPK, PI3K-AKT and Ras-MAPK Pathways

To investigate the effect of metformin on AMPK and on downstream signaling through the PI3K-AKT and Ras-MAPK pathways, we treated Hec1A, Ishikawa, and MecPK cells with metformin (1–10 mM) over 48 hours (Figure 3A). Immunoblotting demonstrated that Hec1A cells expressed PTEN while Ishikawa and MecPK cells had lack of PTEN expression and all cell lines expressed OCT1 (Figure 3B).

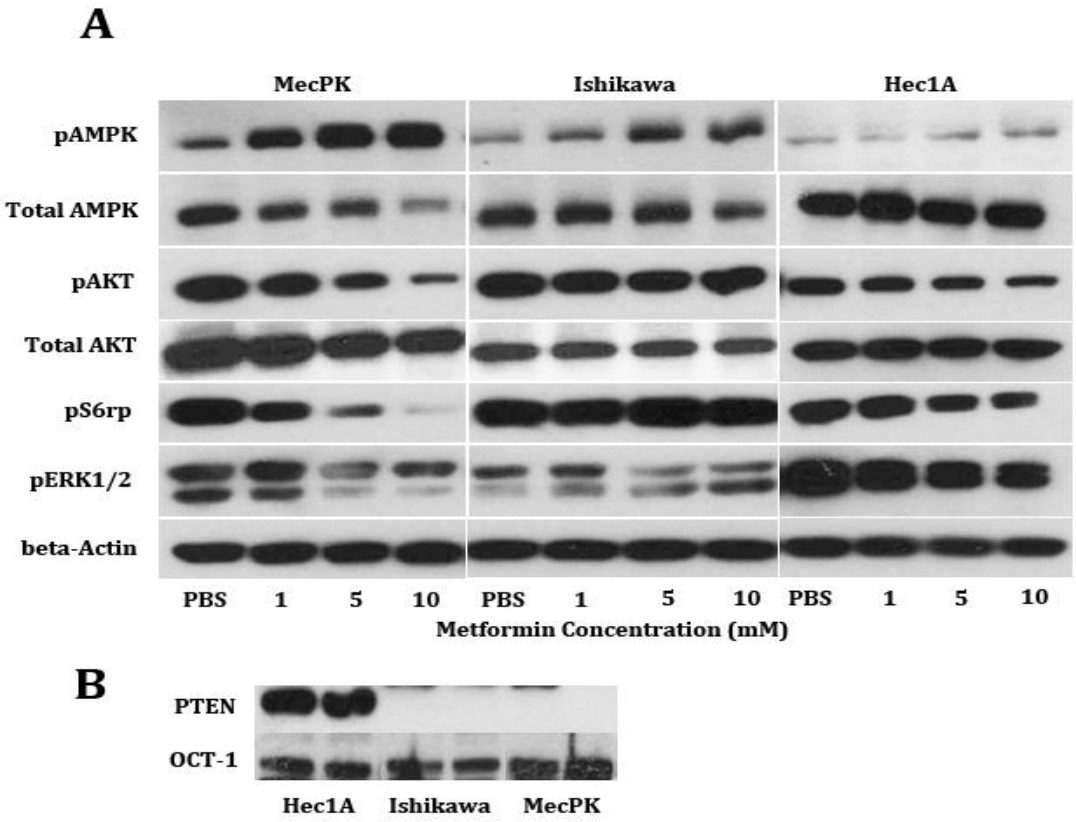

Figure 3. Western immunoblots following metformin treatment - A) Protein expression following metformin treatment after 48 h. In all cell lines, there is an concentration-dependent increase in AMPK activation with metformin treatment. There is a concentration-dependent decrease in pS6rp and pERK1/2 expression in both K-Ras mutant cell lines (Hec1A and MecPK), but not in K-Ras wild-type Ishikawa cells. **B)** PTEN is expressed in Hec1A cells, but not in Ishikawa and MecPK. All cell lines express the organic cation transporter-1 (OCT1) that is required for metformin transport into cells.

Metformin induced phosphorylation of AMPK in a concentration-dependent manner in all cell lines. We next evaluated the effect on metformin on the downstream target of the mTOR pathway, the S6 ribosomal protein (S6rp). While metformin treatment resulted in a concentration-dependent decrease in pS6rp expression in Hec1A and MecPK cells, pS6rp expression was not affected by metformin in Ishikawa cells even at high (10 mM) concentrations. ERK1/2 are downstream targets of the Ras-MAPK pathway. Similar to the effect seen on S6rp, metformin induced a concentration-dependent decrease in phosphorylation of ERK1/2 in Hec1A and MecPK cells, but not in Ishikawa cells indicating that metformin may have an effect on Ras-MAPK signaling in K-Ras mutant cells. Although AKT is upstream of TSC-2 (the direct target of AMPK), metformin treatment resulted in decreased phosphorylation of AKT in both Hec1A and MecPK cells indicating that metformin may also have effects upstream in the PI3K pathway possibly independent of its activity through AMPK. This effect was not seen in Ishikawa cells. Total AKT and total AMPK expression were not affected by metformin in any of the cell lines tested.

3.3. Effect of Metformin on Apoptosis and Cell Cycle Progression

To determine the effect of metformin on apoptosis we evaluated the fraction of cells in the sub-G1 phase as a function of metformin treatment using flow cytometry (Figure 4A). Metformin appears to be a potent inducer of apoptosis in Hec1A and MecPK cells with significant increases in the fraction of apoptotic cells seen at

concentrations of 5 mM ($p<0.001$) and 1 mM ($p=0.048$), respectively. In contrast, metformin did not induce apoptosis in Ishikawa cells.

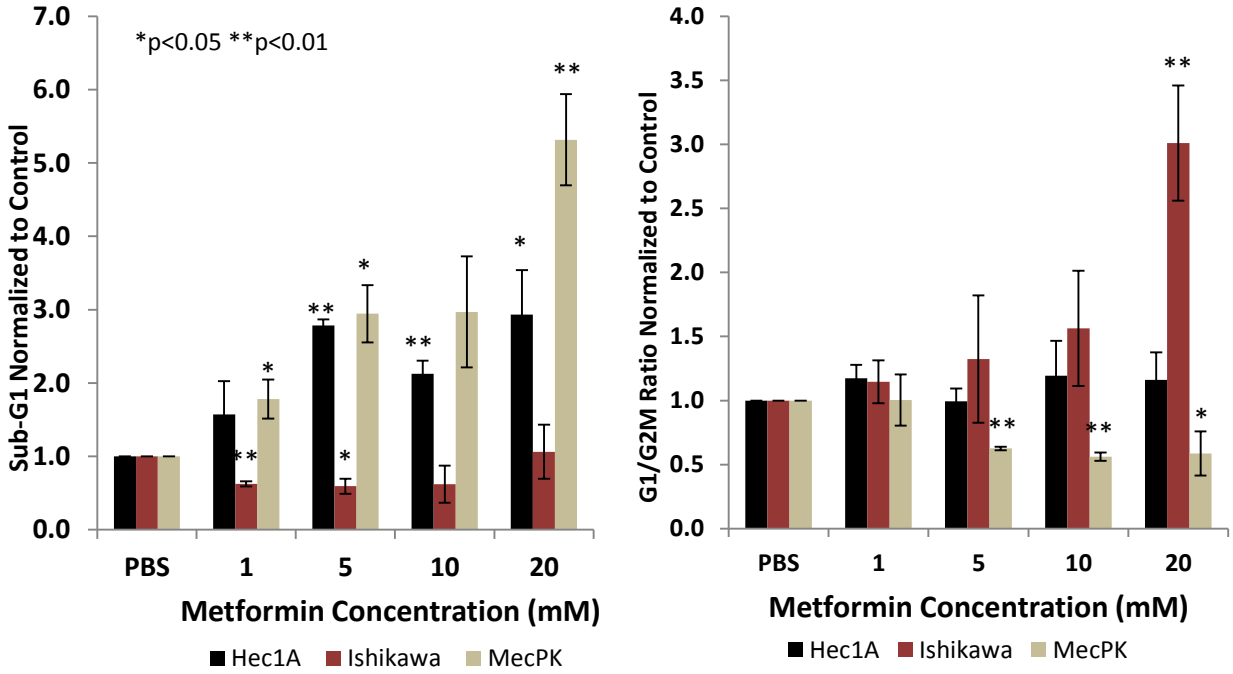

Figure 4. Cell cycle analysis following metformin treatment - A) The proportion of cells in the sub-GI phase following 48h of metformin treatment at increasing concentrations, normalized to control. Metformin significantly induces apoptosis in both Hec1A and MecPK at concentrations as low as 5mM and 1mM, respectively. Metformin does not induce apoptosis in Ishikawa cells. **B)** The ratio of cells in the G1 phase to G2 phase following 48h of metformin treatment at increasing concentrations, normalized to control. While metformin induced a G1 cell cycle arrest in Ishikawa cells at the highest metformin concentration, it induced a concentration-dependent G2/M arrest in MecPK cells. Metformin did not produce a cell cycle arrest in Hec1A cells. These data represent three independent experiments. Error bars indicate +/- SEM.

We also evaluated the effect of metformin treatment on the cell cycle by comparing the ratio of cells in the G1:G2 phase as a function of metformin treatment (Figure 4B). Metformin induces a G2/M arrest in MecPK cells at concentrations as low as 5 mM ($p<0.001$). In contrast, metformin induces a G1 arrest in Ishikawa cells,

but only at the highest drug concentration (20 mM, p=0.003). Metformin does not appear to affect cell cycle progression in Hec1A cells.

3.4. Effect of Metformin on In Vivo Tumor Growth

Following intraperitoneal injection of EC cell lines into athymic nude mice and stratification into metformin-treated and vehicle-treated groups mice were observed for symptoms including massive ascites, hunched posture, or abnormal gait indicating impending death. Each cage (housing 5 mice) consistently drank 25 mL/day regardless of metformin water or control water throughout the course of the study. When at least one mouse in each group was noted to display any moribund symptoms, all mice in the group were euthanized. The time to the development of moribund symptoms was 50 days for the Hec1A group, 64 days for the Ishikawa group, and 29 days for the MecPK group. At the conclusion, all 20 (100%) mice injected with Hec1A, all 20 (100%) mice injected with Ishikawa, and 17 of 20 mice (85%) injected with MecPK developed intraperitoneal tumors. Table 1 provides a summary of results. Prior to necropsy, all mice were weighed. Mean body weights for control and metformin-treated mice were not significantly different for any of the cell lines (Table 1). Following weight determination and collection of serum, necropsy was performed and all visible tumors were collected from all peritoneal surfaces. Metformin-treated mice had a significantly decreased mean tumor weight compared to untreated mice (0.22 g vs. 0.40 g, p=0.002) in the Hec1A group and in the MecPK group (0.722 g vs. 1.372 g, p=0.024). In contrast, there was no difference in mean tumor weights between metformin-treated and untreated mice (0.87 g vs. 1.12 g, p=0.337) in the Ishikawa group. As markers for toxicity, we also

evaluated and compared mean mouse weights at the time of necropsy and serum liver enzyme levels. Mean mouse weights were not significantly different between groups (Table 1). Also, metformin treatment did not adversely affect serum liver enzyme levels (Table 1).

Cell Line	Mice (n)	Developed Tumor n(%)	Time to Moribund (days)	Mean Mouse Wt (g)	Mean Tumor Wt (g)	Mean Serum ALT (U/L)
Hec1A	20	20 (100%)	50	Control: 27.01 Metformin: 25.97 p=0.281	Control: 0.395 Metformin: 0.216 **p=0.002**	Control: 17.5 Metformin: 22.0 p=0.228
Ishikawa	20	20 (100%)	64	Control: 26.28 Metformin: 26.24 p=0.971	Control: 1.119 Metformin: 0.868 p=0.337	Control: 30.0 Metformin: 37.7 p=0.616
MecPK	20	17 (85%)	29	Control: 26.41 Metformin: 24.95 p=0.420	Control: 1.372 Metformin: 0.722 **p=0.024**	Control: 13.7 Metformin: 17.0 p=0.059

Table 2. *In Vivo* effect of metformin on mean tumor weight in nude mouse xenografts. Metformin treatment resulted in significant reductions in mean tumor weights in Hec1A- and MecPK-inoculated mice.

3.5. Effect of Metformin on Tissue Expression of pS6rp and Ki-67

Immunohistochemical analysis of tumor pS6rp expression as a downstream marker of PI3K/AKT pathway signaling and Ki-67 staining as a marker for proliferation was carried out. The mean percentage of cells staining positive for Ki-67 was not significantly different between metformin-treated and vehicle control-treated groups for either Hec1A or Ishikawa tumor tissues (Figure 5A). However, consistent with the *in vitro* results, expression of pS6rp was significantly decreased

in metformin-treated Hec1A tumor tissue compared to vehicle control-treated tissue (mean IHC score 4.9 vs. 7.8, p=0.009) – (Figure 5B). In contrast, there was no significant difference in the expression of pS6rp in metformin-treated Ishikawa tumor tissue compared to vehicle control-treated tissue (mean IHC score 5.8 vs. 5.3, p=0.642) – (Figure 5B).

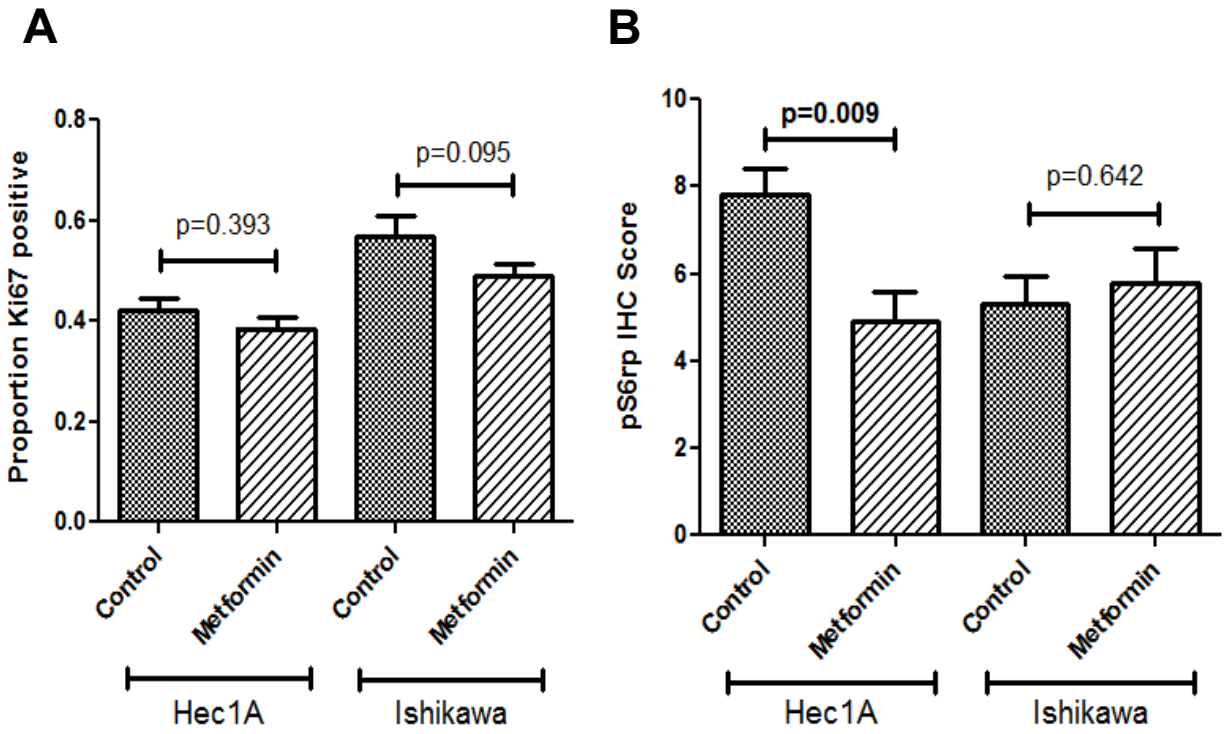

Figure 5. Immunohistochemical analysis of xenograft tumors - A) There were no differences in the percentage of cells staining positive for Ki-67 between metformin-treated and vehicle control-treated groups for either Hec1A or Ishikawa tumor tissues. **B)** Expression of pS6rp was significantly decreased in metformin-treated Hec1A tumor tissue compared to vehicle control-treated tissue

3.6. Expression of PTEN Does Not Alter Response to Metformin

Transfection of MecPK cells with plasmid pIRES2 containing PTEN gene insert resulted in stable expression of PTEN. The functionality of PTEN was confirmed by evaluating the activation of downstream signaling pathways; pS6rp expression was

down-regulated in PTEN expressing cells as compared to MecPK cells transfected with plasmid alone (Figure 6A). Following metformin treatment for 48 hours at varying concentrations, there was no difference in relative cell viability when comparing parental MecPK transfected with pIRES2-vector alone to MecPK cells transfected with pIRES2-EGFP-PTEN stably expressing PTEN (Figure 6B). The mean IC50 value for control MecPK cells was 3.31 mM and for MecPK cells expressing PTEN it was 3.00 mM.

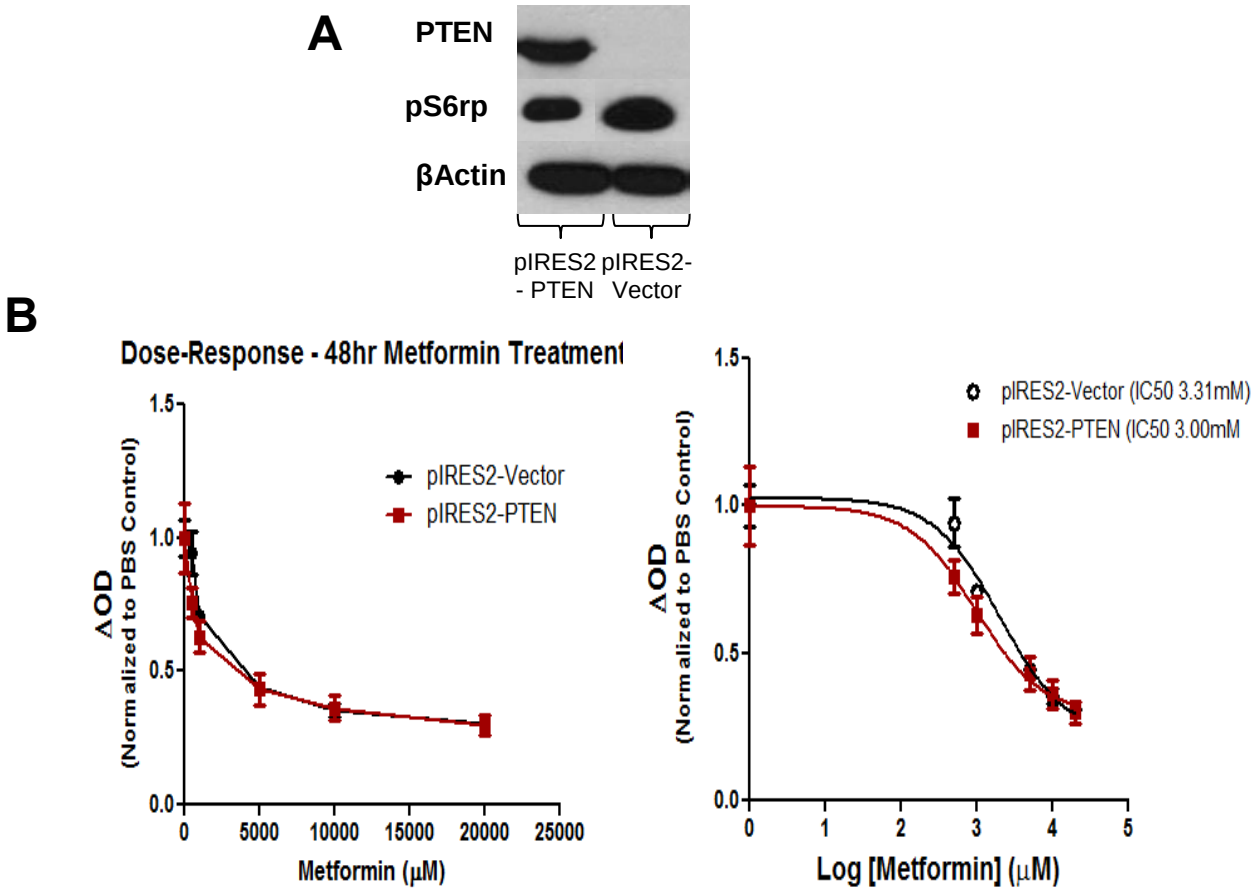

Figure 6. Re-expression of PTEN in MecPK cells and dose-response to metformin treatment - A) Transfection of MecPK cells with plasmid pIRES2-EGFP-PTEN insert demonstrated expression of PTEN which resulted in down-regulation of downstream read-out pS6rp compared to MecPK cells transfected with pIRES2-EGFP-vector alone. **B**) Following metformin treatment for 48 h, there were no significant differences relative cell viability between parental MecPK and cells expressing PTEN. These data represent three independent experiments performed in triplicate. Error bars indicate +/- SEM.

3.7. Transient Silencing of Mutant K-Ras Decreases Sensitivity to Metformin Treatment

Transient silencing of K-Ras in MecPK cells using targeted siRNA results in a significantly decreased expression of total K-Ras when compared to cells treated with non-target siRNA (control) (Figure 7A). In both groups, metformin treatment at 5 – 20 mM resulted in significant decreases in relative cell survival compared to PBS-treated controls indicating that K-Ras silencing alone is not sufficient to abrogate metformin's effect on proliferation. However, cells with transiently silenced K-Ras demonstrated significantly decreased sensitivity to metformin treatment (5 – 20 mM) compared to parental MecPK cells transfected with non-targeted siRNA (Figure 7B).

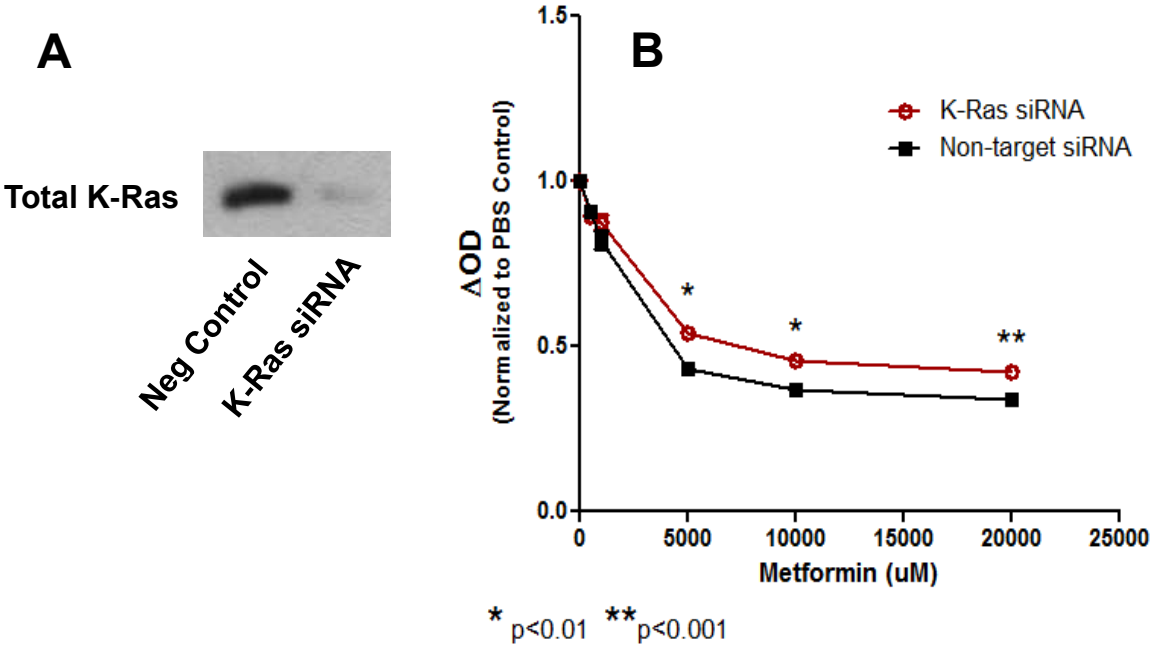

Figure 7. Transient silencing of K-Ras in MecPK cells and dose-response to metformin treatment - A) Transient silencing of K-Ras in MecPK cells using targeted siRNA results in decreased total K-Ras expression. **B)** Following treatment for 48 h, MecPK cells with transiently silenced K-Ras displayed decreased sensitivity to metformin at 5 – 20 mM compared to parental MecPK cells transfected with non-targeted siRNA (negative control). These data represent three independent experiments performed in triplicate. Error bars indicate +/- SEM.

3.8. Expression of Mutant K-Ras Increases Sensitivity to Metformin Treatment

Transfection of Ishikawa cells with plasmid pMEV containing an oncogenic mutant K-RasG12D insert resulted in a 4-fold increased expression of K-Ras at the mRNA level when compared to Ishikawa cells transfected with pMEV vector alone (Figure 8A). Following metformin treatment for 48 hours at varying concentrations, cells expressing the mutant K-Ras had slightly increased sensitivity to metformin compared to controls expressing wild-type K-Ras. IC50 values for the controls could not be calculated based on concentrations used and the dose-response curve. However, a metformin IC50 of 57.7 mM was calculated in Ishikawa cells expressing mutant K-Ras (Figure 8B).

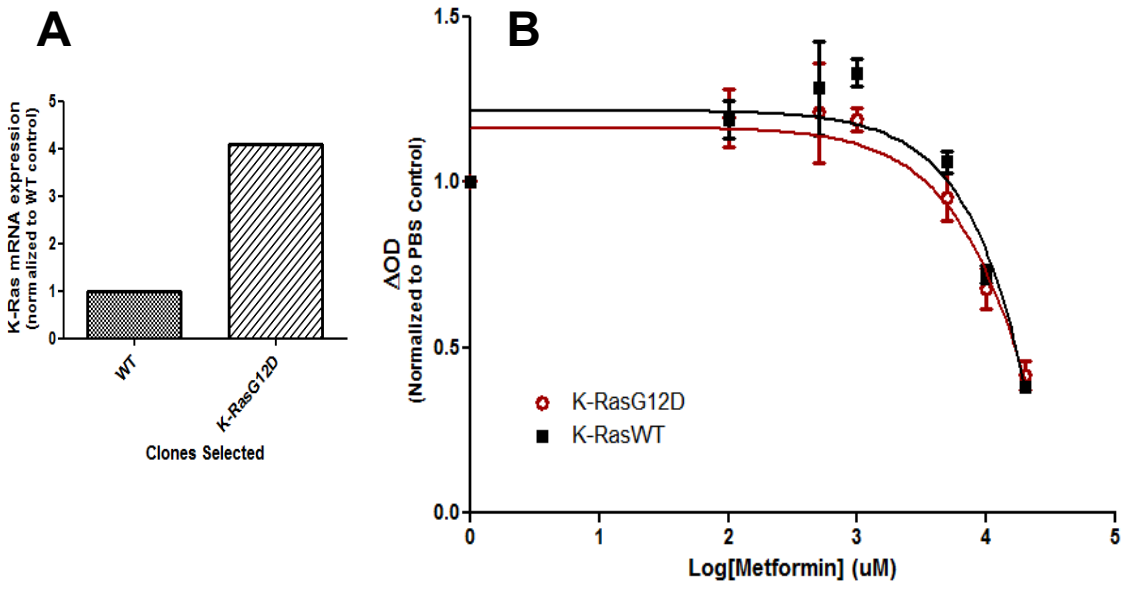

Figure 8. Expression of mutant K-RasG12D in Ishikawa cells and dose-response to metformin treatment - A) Transfection of Ishikawa cells with plasmid pMEV containing an oncogenic mutant K-RasG12D insert resulted in a 4-fold increased expression of K-Ras at the mRNA level. **B)** Cells expressing the mutant K-Ras had slightly increased sensitivity to metformin compared to controls expressing wild-type K-Ras following 48h of treatment. These data represent three independent experiments performed in triplicate. Error bars indicate +/- SEM.

3.9. Metformin Treatment Causes Mislocalization of K-Ras to the Cytoplasm

Confocal microscopy analysis was used to evaluate the localization of GFP-K-RasG12V (Figure 9A) and GFP-H-RasG12V (Figure 9B) in MDCK cells in response to increasing concentrations of metformin over 48 hours.

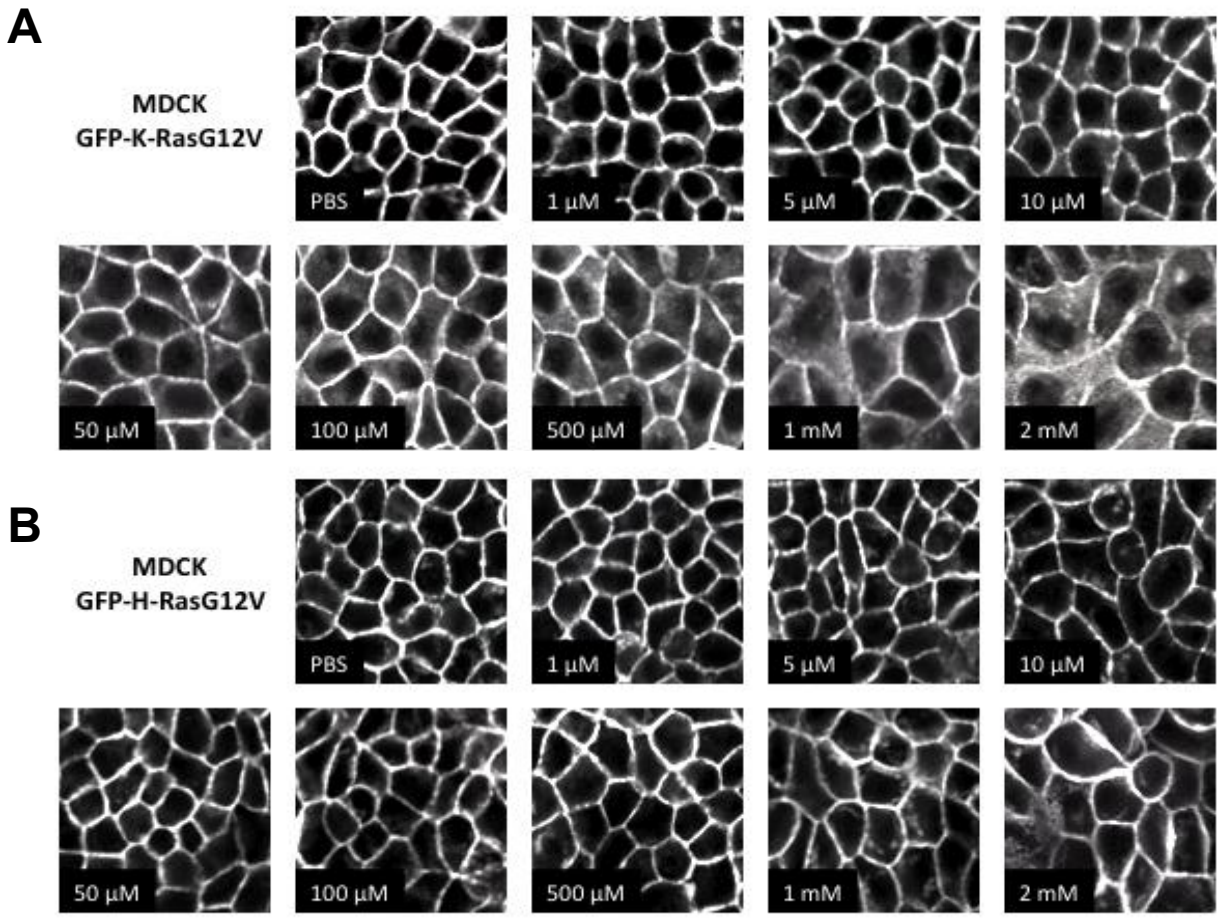

Figure 9. Effect of metformin (0.001 – 2 mM) on K-Ras localization analyzed by confocal microscopy in Madin-Darby Canine Kidney (MDCK) cells - Expressing **A)** GFP-labeled oncogenic K-RasG12V mutant and **B)** GFP-labeled oncogenic H-RasG12V mutant.

MDCK cells expressing GFP-K-RasG12V treated with metformin showed a concentration-dependent translocation of K-Ras from the plasma membrane to the cytoplasm, with an IC50 of 357 uM (Figure 10). In contrast, in MDCK cells expressing GFP-H-RasG12V, translocation of H-Ras from the plasma membrane to the cytoplasm was less sensitive to metformin treatment, with an IC50 of 2.76 mM (Figure 10). The advantage to using MDCK cells for this screening assay is that they grow in confluent monolayers allowing for clear imaging and analysis.

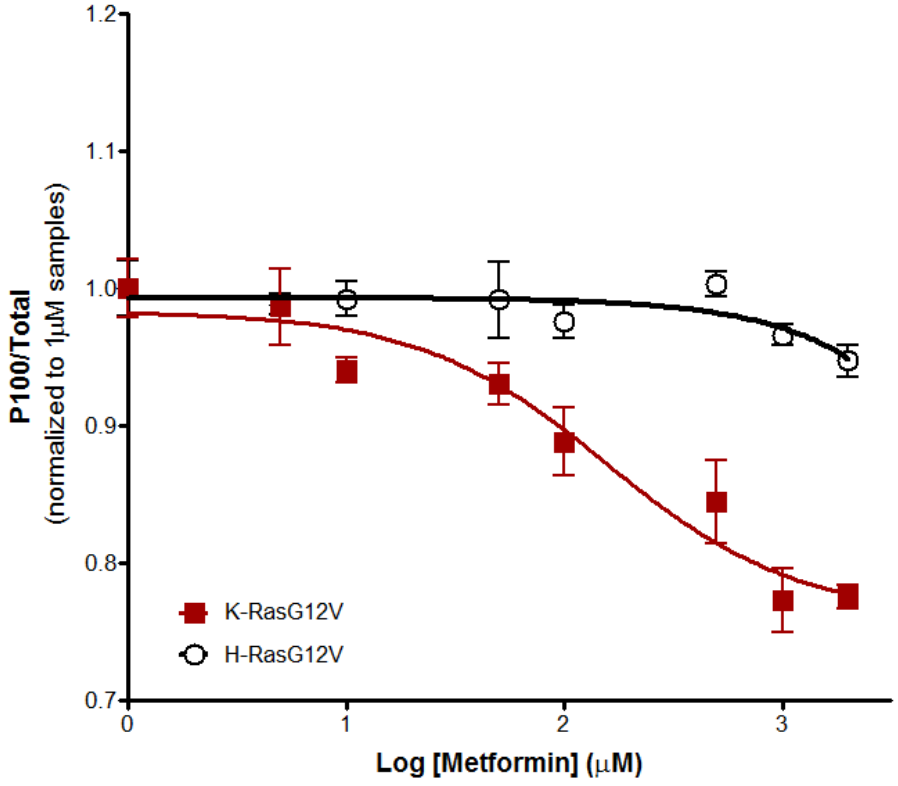

Figure 10. Quantitative analysis of K-Ras and H-Ras localization following metformin treatment using confocal microscopy. Treatment with metformin resulted in a concentration-dependent translocation of K-Ras from the plasma membrane to the cytoplasm, with a mean IC50 of 357 uM. These data represent three independent experiments performed in triplicate. Error bars indicate +/- SEM.

We attempted to validate the results observed above in human endometrial cancer (Hec1A) cells transfected with GFP-K-RasG12V (Figure 11). However, as Hec1A cells have a tendency to grow in multiple layers when confluent, this made quantification of intracellular localization using confocal microscopy unreliable.

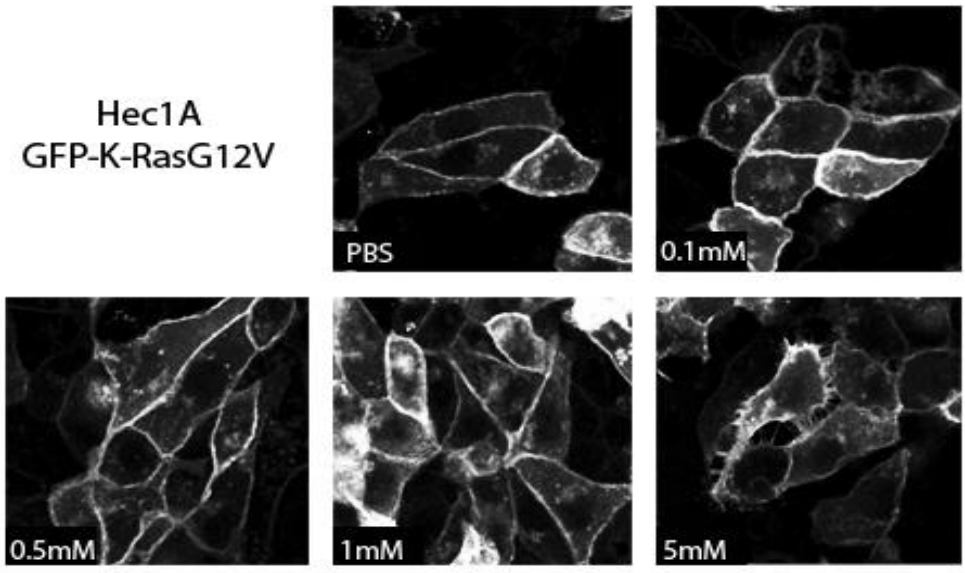

Figure 11. Effect of metformin (0.1 – 5 mM) on K-Ras localization analyzed by confocal microscopy in Hec1A cells expressing GFP-labeled oncogenic K-RasG12V mutant.

As a result, metformin's effect on K-Ras localization was validated using in Hec1A cells by subcellular fractionation studies and western immunoblot analysis. To confirm purity of cellular fractions and equal loading of proteins, membranes were incubated with antibodies directed against Na+/K+ ATPase (membrane-specific) and total AKT (cytoplasm-specific) – (Figure 12A). Metformin treatment caused a concentration-dependent mislocalization of K-Ras from the plasma membrane to the

cytoplasm with significance achieved at 1 and 5 mM of metformin (p=0.006 and p<0.001) compared to PBS treatment (Figure 12B).

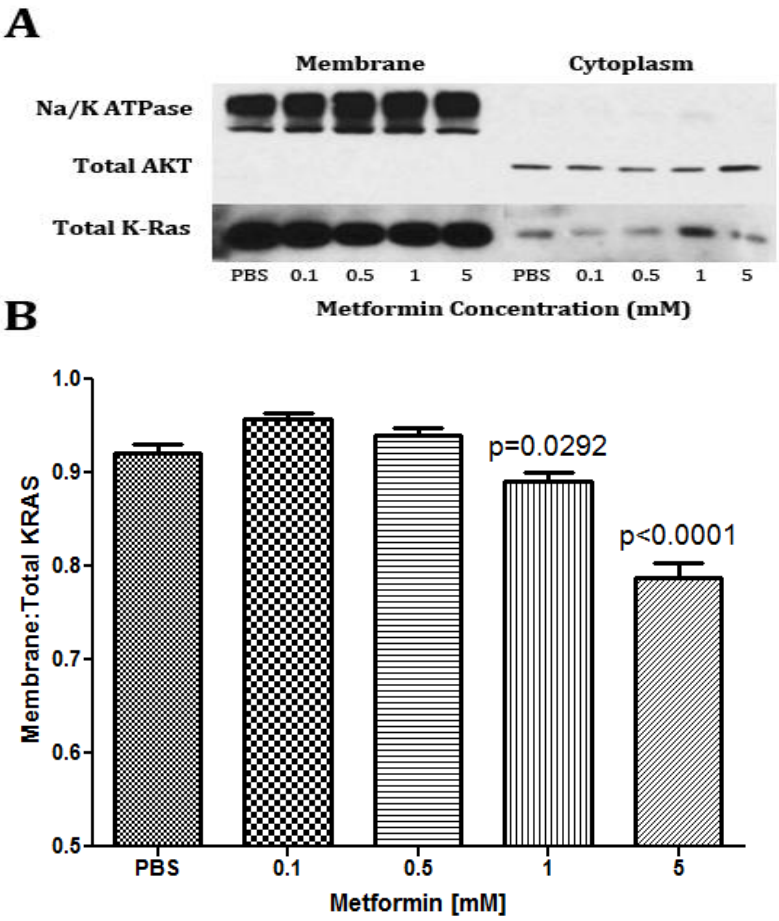

Figure 12. Hec1A subcellular fractionation following metformin treatment - A) Na/K ATPase served as the membrane-specific antibody and Total AKT served as the cytoplasm-specific antibody to confirm purity of fractions. **B)** Metformin treatment induced a concentration-dependent translocation of K-Ras from the plasma membrane to the cytoplasm with significance achieved at 1 and 5 mM (p=0.029 and p<0.0001) compared to PBS treatment. These data represent three independent experiments performed in triplicate. Error bars indicate +/- SEM.

3.10. The Effect of Metformin on K-Ras Localization is AMPK-Independent

Treatment of Hec1A cells with AICAR resulted in a concentration-dependent mislocalization of K-Ras from the plasma membrane to the cytoplasm with significance at 0.1 mM (p=0.0002) and 1 mM (p<0.0001) – Figure 13A and 13B. To evaluate whether this effect is AMPK-dependent, we pretreated cells with Compound C 10 uM for 1 hour prior to and during treatment with metformin or AICAR. The addition of Compound C did not result in a significant difference in K-Ras mislocalization following treatment with metformin 5 mM (p=0.257) or with AICAR 1 mM (p=0.946) – Figure 14B.

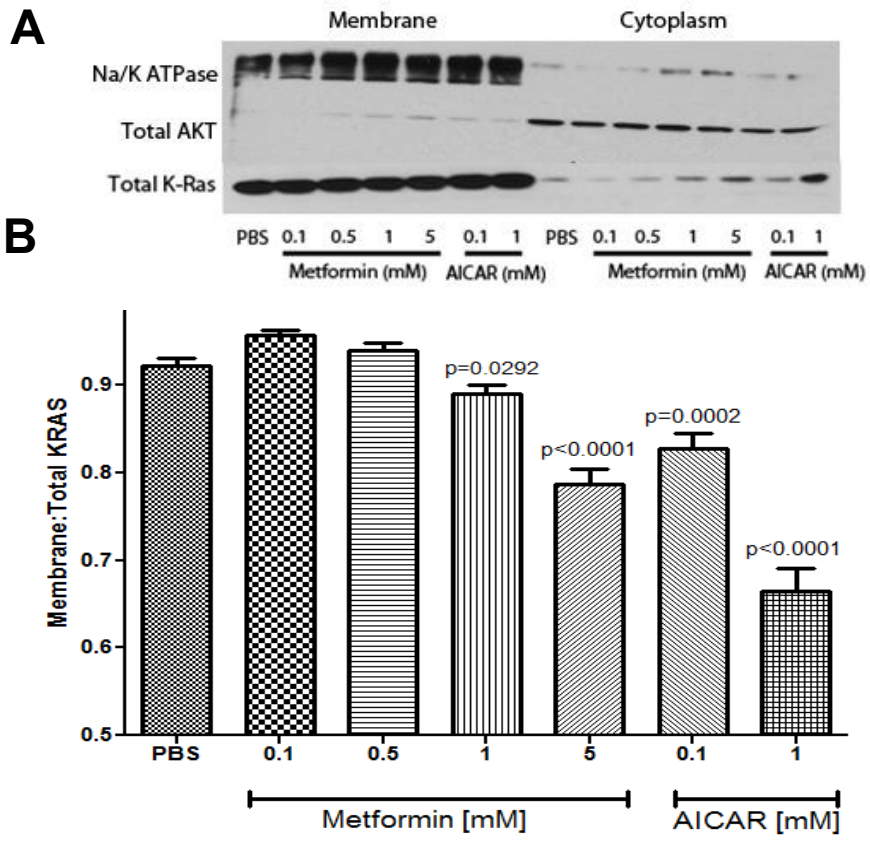

Figure 13. A) Hec1A subcellular fractionation following 48 h of metformin or AICAR treatment. **B)** AICAR also induced a concentration-dependent translocation of K-Ras from the plasma membrane to the cytoplasm compared to PBS treatment. These data represent two independent experiments performed in triplicate. Error bars indicate +/- SEM.

To confirm whether compound C had an effect on AMPK activation over this extended course of treatment, western immunoblotting was performed during which membranes were incubated with antibody directed against phosphorylated AMPKα (Thr172) (pAMPKα). Cells treated with Compound C exhibited decreased expression of pAMPKα at both the membrane and in the cytoplasm when compared to cells that were not treated with Compound C (Figure 14A). This indicates that the effects of metformin and AICAR on K-Ras mislocalization are AMPK independent.

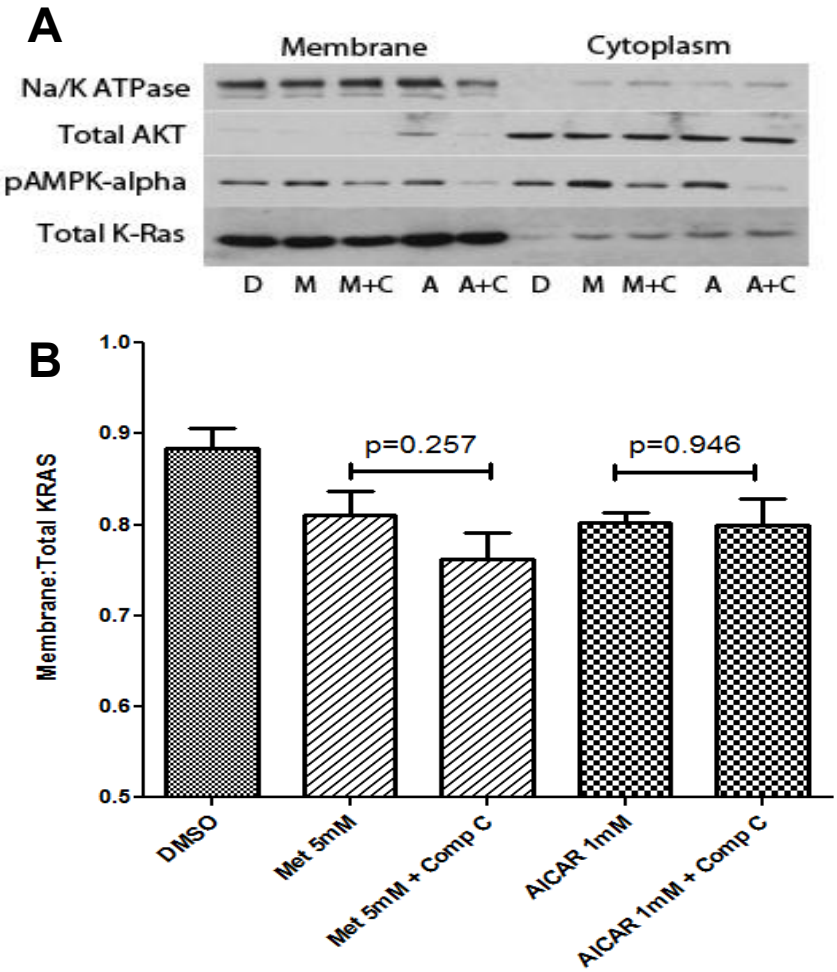

Figure 14. Hec1A subcellular fractionation following 48 h of metformin or AICAR treatment with and without Compound C – A) Treatment with Compound C resulted in decreased expression of pAMPKα. **B)** Pre-treatment with Compound C 10 uM for 1 hour followed by co-treatment with either Metformin 5 mM or AICAR 1 mM did not alter the effect of these drugs on K-Ras localization. These data represent two independent experiments performed in triplicate. Error bars indicate +/- SEM. *D – DMSO; M – Metformin 5 mM; A – AICAR 1 mM; C – Compound C 10 uM*

3.11. The Combination of Metformin with PI3K Pathway Inhibitors Results in an Additive Decrease in Cell Viability

The relative cell viability of MecPK cells was determined by MTT assays after 48 hours of the following treatments: RAD001 10 nM, BEZ235 100 nM, metformin 5 mM, AZD6244 10uM, and the combinations of RAD001 10 nM plus metformin 5 mM, BEZ235 100 nM plus metformin 5 mM, and AZD6244 10 uM plus metformin 5 mM. The combination of RAD001 with metformin produced a significant decrease in relative cell viability than that achieved with either RAD001 alone ($p=0.008$) or metformin alone ($p=0.035$) – Figure 15A. Similarly, the combination of BEZ235 with metformin produced a significant decrease in relative cell viability than that achieved with either BEZ235 alone ($p=0.003$) or metformin alone ($p=0.029$) – Figure 15B. In contrast, the combination of AZD6244 with metformin did result in a significant decrease in relative cell viability than that achieved with AZD6244 alone ($p=0.201$) or metformin alone ($p=0.661$) – Figure 15C.

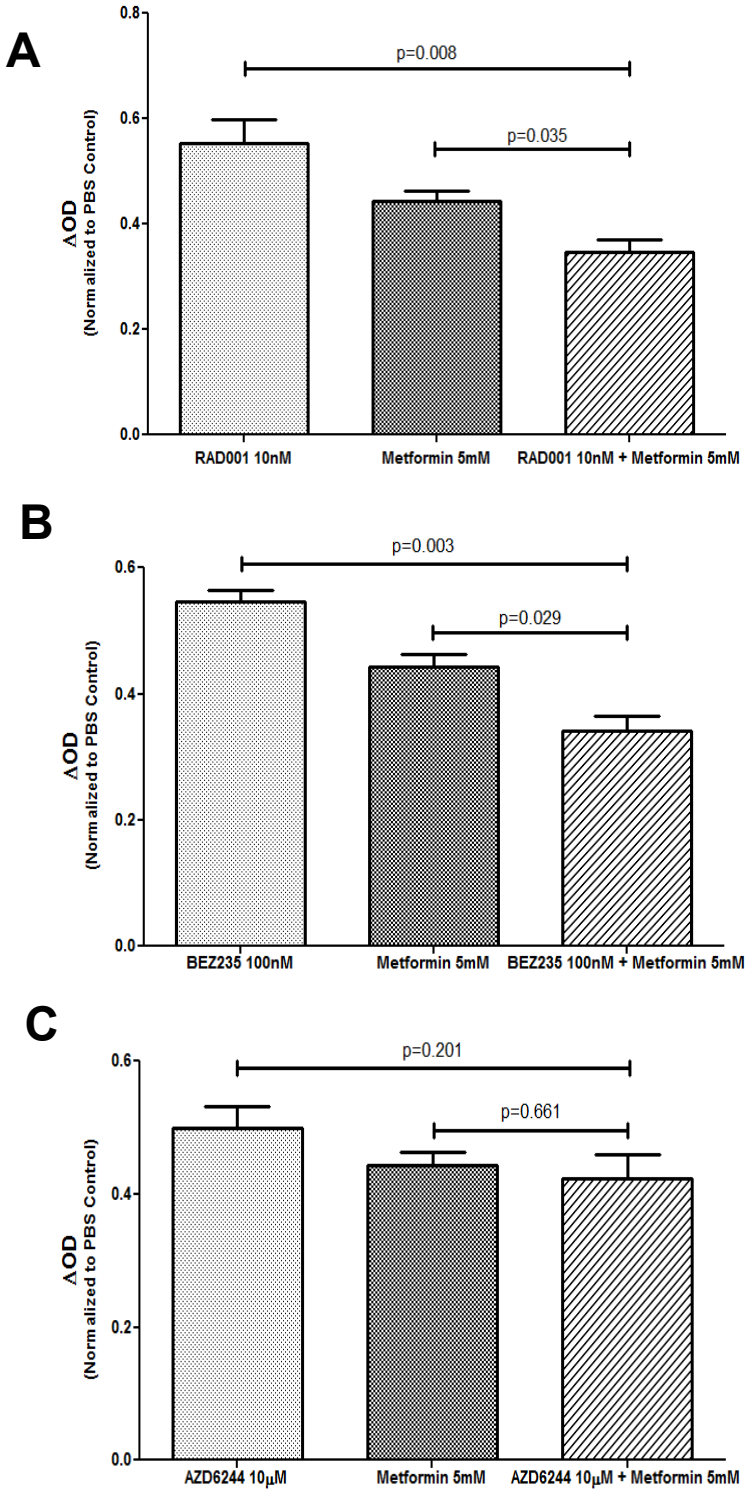

Figure 15. MTT assays representing treatment of MecPK cells with either: **A)** RAD001 10nM or metformin 5mM alone or in combination; **B)** BEZ235 100nM or metformin 5mM alone or in combination; and **C)** AZD6244 10uM or metformin 5mM alone or in combination. For both RAD001 and BEZ235, combination treatment with metformin resulted in decreased relative cell viability than with either agent alone. In contrast, combination treatment with the MEK inhibitor AZD6244 and metformin did not result in a greater decrease in relative cell viability than with either agent alone. These data represent three independent experiments performed in triplicate. Error bars indicate +/- SEM.

The expression of downstream proteins in the PI3K and Ras-MAPK pathways were evaluated by western immunoblots following treatment with DMSO, metformin 5 mM, RAD001 10 nM, AZD6244 6 uM, or the combinations of RAD001 10 nM plus metformin 5 mM or RAD001 10 nM plus AZD6244 6 uM. Treatments and immunoblots were performed on MecPK cells and expressed in Figure 16. Metformin treatment increased the expression of pAMPKα and decreased the expression of pAKT, pS6rp, and pERK1/2. These effects were more prominent in cells treated with the combination of RAD001 and metformin. Treatment with AZD6244 increased the expression of pAKT and pS6rp. Following the addition of RAD001 to AZD6244, pS6rp expression decreased, but pAKT remained overexpressed compared to DMSO treated cells.

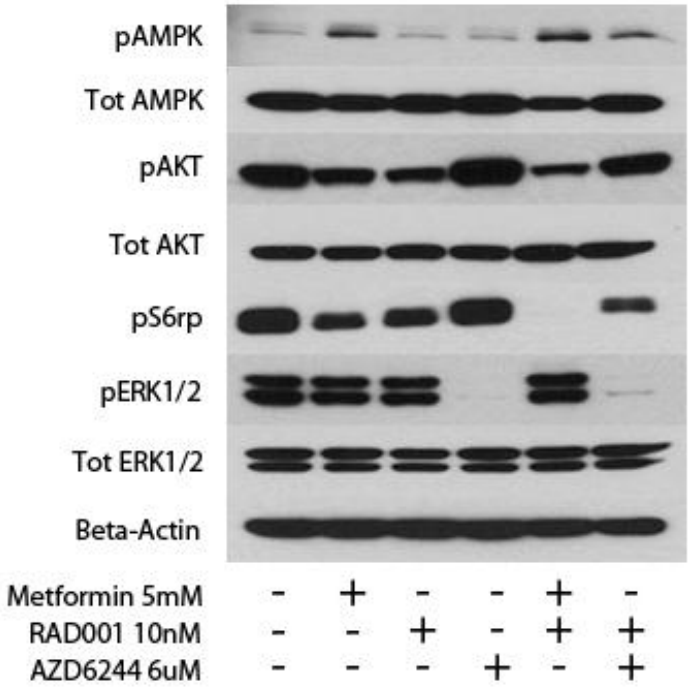

Figure 16. MecPK cells treated for 48h with metformin 5 mM alone, RAD001 10 nM alone, AZD6244 6 uM alone, or combinations of RAD001 with either metformin or AZD6244. Metformin treatment increased the expression of pAMPKα and decreased the expression of pAKT, pS6rp, and pERK1/2. These effects were more prominent in cells treated with the combination of RAD001 and metformin.

Similarly, addition of metformin 5 mM to BEZ235 100 nM resulted in decreased expression of pS6rp and pAKT (Figure 17). BEZ235 alone does not appear to affect MAPK signaling (pERK1/2 expression). However, metformin alone and in combination with BEZ235 treatment decreases pERK1/2 expression.

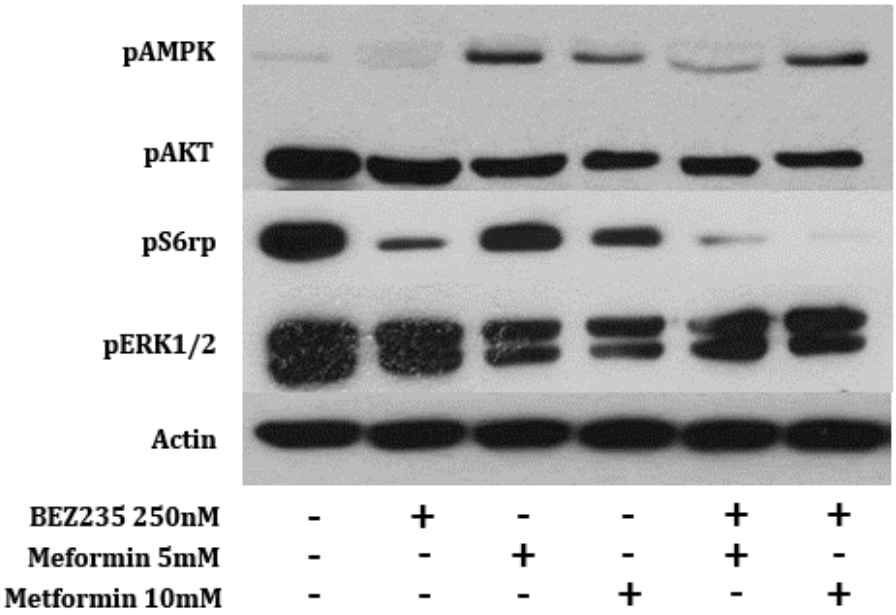

Figure 17. Addition of metformin to BEZ235 results in decreased phosphorylation of S6rp and AKT. BEZ235 alone does not appear to affect pERK1/2 expression (Ras-MAPK pathway). However, metformin alone and in combination with BEZ235 treatment decreases Ras-MAPK signaling.

4. Discussion

The chemopreventive and antineoplastic effects of metformin are currently being evaluated for the treatment of a variety of cancers. Although its mechanism of action is not fully understood, metformin is thought to inhibit cell proliferation locally via activation of the AMPK signaling pathway, which counteracts the growth-promoting effects of PI3K pathway hyperactivity. Activation of the PI3K pathway, as a consequence of the inactivating mutation of the PTEN tumor suppressor gene, is a commonly observed mutation in type I endometrial cancer. With this in mind, we set out to evaluate the *in vitro* and *in vivo* effects of metformin on endometrial cancer growth based on PTEN mutational status. While we demonstrated that metformin is a potent inhibitor of cell proliferation and inducer of apoptosis *in vitro* and of tumor growth *in vivo*; surprisingly its activity appears to be more robust in endometrial cancer cell lines that possess an activating K-Ras mutation as compared to those lacking PTEN. These preliminary findings led us to further evaluate the effect of metformin on Ras signaling and intracellular localization.

First, we confirmed metformin activates AMPK in a concentration-dependent manner in all endometrial cancer cell lines used. A decrease in PI3K pathway signaling was observed in Hec1A and MecPK cells, both of which harbor activating mutations in K-Ras, but not in Ishikawa cells which express wild-type K-Ras. Furthermore, we demonstrated that pERK1/2 expression was decreased in a concentration-dependent manner only in Hec1A and MecPK cells and observed that metformin is a potent inducer of apoptosis in both of these cell lines. These *in vitro* findings were further supported by our xenograft model which demonstrated reduced

tumor growth in metformin-treated mice that had been inoculated with Hec1A or MecPK, but not with Ishikawa.

Based on these data, a few other observations can be made. Metformin can produce anti-proliferative effects *in vitro* indicating that it acts directly on endometrial cancer cells and is not solely reliant on reducing serum insulin levels. It is noteworthy that the effects of metformin on *in vivo* tumor growth mirrored the effects seen *in vitro*. Certainly, this is not to minimize the proposed indirect mechanism of action of metformin, but, rather, indicates that the anti-neoplastic actions of metformin on endometrial cancer likely represent a combination of both direct and indirect effects. Importantly, all endometrial cancer cell lines included in this study expressed OCT1. OCT1 or OCT3 have previously been demonstrated to be essential for metformin entry into cells. Indeed, cells that do not express OCT1 are immune to the direct effects of metformin (42). In a recent study evaluating the relevance of the OCT1 transporter to the antineoplastic effect of biguanides in epithelial ovarian carcinoma (EOC), siRNA knockdown of OCT1 reduced the sensitivity of EOC cells and abrogated the activation of AMPK in response to metformin in a concentration-dependent manner (42).

A frequently cited criticism of preclinical studies involving metformin is that concentrations used *in vitro* are higher than therapeutic serum concentrations achieved in clinical practice. Specifically, across various cancer cell lines, IC50s achieved with metformin are in the millimolar range (1-10 mM), while the therapeutic serum concentration of metformin in diabetic patients (treated with 500-2000 mg/day orally) is approximately 20 mcmol/mL. Although this appears to be quite a

difference, there are a few possible explanations. First, the media used in tissue culture often contains supraphysiologic glucose levels that may limit the response to metformin (99). Also, metformin has been shown to accumulate in tissues at concentrations significantly higher than in the serum in both mice (38) and human studies (39). Using a formula for dose translation from human to mouse based on body surface area (BSA) (100), a standard human metformin dose of 24.3 mg/kg daily (based on 850 mg twice daily by mouth in a 70 kg human) translates to 299.7 mg/kg daily in a mouse. In our metformin xenograft study, each mouse was treated daily with 5 mg of metformin dissolved in drinking water. Assuming an average mouse weight of 0.02 kg, each mouse received 250 mg/kg of metformin daily which is similar, and certainly not higher, to what is expected based on human equivalency dosing. Furthermore, in our xenograft model, metformin did not induce weight changes or elevations in serum liver enzymes that would indicate toxicity.

While our preliminary data provided some insight into specific genetic alterations that may make a cell more sensitive to metformin treatment, we next sought to evaluate if metformin's antiproliferative effects are mediated specifically by opposing the Ras-MAPK or PI3K signaling pathways, or both. Furthermore, we sought to determine if the mechanism of inhibition is something other than up-regulation of AMPK by disruption of the energy homeostasis of the cell. First, to investigate the role of PTEN expression on the activity of metformin, we stably transfected and re-expressed PTEN in MecPK cells and compared their response to metformin with MecPK cells transfected with vector alone. As you may recall, MecPK cells are derived from a transgenic mouse harboring a K-RasG12D mutation and

homozygous loss of PTEN function. In this cell line, we demonstrated that PTEN re-expression does not alter response to metformin. That is, MecPK cells expressing PTEN were not more or less sensitive to metformin treatment by cell viability assays when compared to control MecPK cells with loss of PTEN. In contrast, when K-Ras is transiently silenced in MecPK cells using siRNA, we demonstrated that these cells are less sensitive to metformin at higher concentrations than parental controls. These observations indicate that metformin may act to disrupt signaling of the Ras-MAPK pathway, a well-known pro-survival pathway that is frequently mutated in a variety of tumor types. The next question was: How?

As described above, Ras signaling requires a series of post-translational modifications with the ultimate goal of facilitating transport of the Ras protein to the plasma membrane where, in response to growth signals, it is activated by GEFs and can interact with effector molecules to propagate the growth signal. Mutations in Ras lead to constitutive activation and persistent signaling through effector pathways which can ultimately lead to malignant transformation. We have already reviewed the extensive cross-talk between the Ras and PI3K pathways and the importance of the latter in Ras-dependent tumor initiation and maintenance. This process is further accentuated by frequently encountered activating mutations in the PI3K pathway, such as PIK3CA mutations or PTEN loss of function. Interestingly, while mutations in the Ras and PI3K pathways are mutually exclusive in some tumor types such as breast cancer, they frequently coexist in endometrial and colon cancer (48, 81, 85, 101). Given our preliminary results demonstrating that metformin appeared to have the greatest inhibitory effect on cellular proliferation and *in vivo* tumor growth in

endometrial cancer cell lines harboring activating K-Ras mutations regardless of PTEN expression status; we hypothesized that metformin may have a direct effect on K-Ras localization and trafficking to the plasma membrane, leading to decreased activation and subsequent decreased signaling through effector pathways. Following a series of experiments evaluating the subcellular localization of Ras in response to metformin treatment, we demonstrated that metformin causes mislocalization of Ras from the plasma membrane to the cytoplasmic compartment. This effect appears to be specific to the K-Ras isoform as mislocalization of H-Ras to the cytoplasm required much higher metformin concentrations. This indicates that metformin acts to disrupt transport of Ras proteins, in other words the "second signal," rather than altering or inhibiting the series of post-translational modifications required for all newly synthesized Ras proteins to localize to the Golgi.

The interaction between metformin and the Ras-MAPK signaling pathway have gained increasing attention recently. Metformin has been shown to inhibit Ras-induced reactive oxygen species production and DNA damage; a mechanism that may contribute to its effects as a cancer preventive agent (102). In breast cancer, metformin has been demonstrated to induce cancer cell apoptosis by targeting ERK signaling (103). However, what has yet to be reported is the mechanism by which metformin disrupts Ras signaling. Our data suggests that metformin may disrupt plasma membrane localization of K-Ras and hence its signaling. As K-Ras and H-Ras are transported to the plasma membrane through different mechanisms, metformin, through an unclear mechanism, interferes specifically with K-Ras transport. This may possibly occur through disruption of electrostatic interactions

between K-Ras and the plasma membrane or through activation of a farnesyl-electrostatic switch. In the latter, phosphorylation of the polybasic domain of K-Ras by protein kinase C (PKC), or potentially by AMPK, reduces the net positive charge, causing K-Ras to lose affinity to the plasma membrane and to accumulate in endomembranes (57). Interestingly, it has been demonstrated that when K-Ras has an activating mutation, translocation to endomembranes is associated with apoptosis (104). This may further explain our findings that metformin potently induces apoptosis in endometrial cancer cell lines harboring an activating K-Ras mutation. To determine if these effects are related to metformin's ability to activate AMPK, we performed a series of experiments using AICAR, an AMP analog that potently activates AMPK, and Compound C, an inhibitor of AMPK. We demonstrated that similar to metformin, AICAR causes concentration-dependent mislocalization of K-Ras to the cytoplasm. However, treatment with Compound C and subsequent inhibition of AMPK did not abrogate the effects of either metformin or AICAR on K-Ras intracellular localization. This indicates that metformin's effects on K-Ras localization are AMPK-independent. Further studies are necessary to investigate the precise mechanism by which metformin causes mislocalization of K-Ras. It has been demonstrated that interference of electrostatic interactions by a cationic amphiphilic drug (chlorpromazine) reduces the association of K-RasG12V (but not H-Ras) with the plasma membrane, leading to accumulation in endosomal or mitochondrial membranes resulting in growth inhibition and apoptosis (105). As metformin exists primarily as a hydrophilic cationic molecule at physiological pH values and has previously been demonstrated to increase the activity of atypical

PKC (34, 106), this may be a possible explanation for its effects on K-Ras mislocalization.

It is also intriguing to speculate on the role of metformin on cancer cell metabolism. Since the 1920s, it has been observed that cancer cells shift from mitochondrial oxidative phosphorylation and rely on glycolysis to generate energy needed for maintenance of cellular processes and growth, a phenomenon known as the “Warburg effect” (107). Most cells in a multicellular organism under normal physiologic conditions rely on mitochondrial oxidative phosphorylation as the energy yield in the form of ATP (36 mol per glucose molecule) is significantly greater than with glycolysis (2 mol of ATP per glucose molecule). As such, these cells reserve glycolysis for conditions of oxygen deprivation allowing cells to continue ATP production. Why is it then that cancer cells preferentially utilize a less efficient metabolic pathway? For one, many cancer cells in solid tumors are in a chronic hypoxic environment demanding that they use anaerobic glycolysis as a means to generate energy. However, even when oxygen is plentiful, cancer cells still preferentially utilize aerobic glycolysis. The reason for this is a shift in their priorities. Cancer cells want to divide rapidly which requires that they replicate all of their cellular contents, a process that requires significantly more resources (such as NADPH and acetyl-coenzyme A) than just ATP alone (107). As such, cancer cells preferentially metabolize glucose and glutamine to generate the precursors needed for fatty acid and amino acid synthesis. Recent work has demonstrated that Ras-dependent transformation results in an early switch to aerobic glycolysis (108, 109). Despite the switch to glycolysis, some cancer cells retain the capacity for oxidative

phosphorylation, particularly when nutrients are low (110). Metformin is known to inhibit oxygen consumption and mitochondrial complex I (111, 112). This inhibition of oxidative phosphorylation may lead to ATP depletion and an energy crisis with the end result of apoptosis. This may provide another explanation for the induction of apoptosis that we demonstrated following metformin treatment in K-Ras mutant cell lines.

Our observations have important clinical implications in endometrial cancer, particularly endometrioid-type, as up to 26% harbor activating K-ras mutations and up to 83% of cases have PTEN loss with subsequent PI3K hyperactivation. With the recent interest in personalizing cancer care, several targeted strategies have been developed and evaluated for the treatment of endometrial carcinoma (113). Unfortunately, some combination therapies involving PI3K pathway inhibitors with MEK inhibitors have proven to be toxic in Phase I studies making their development into feasible treatment strategies uncertain. To evaluate the role of metformin, as a possible Ras-MAPK pathway inhibitor, we combined it with either RAD001 (an mTORC1 inhibitor) or BEZ235 (a pan-PI3K/mTOR inhibitor) and demonstrated decreased relative cell viability on proliferation assays with the combinations than with either of the agents alone. In contrast, when metformin was combined with a MEK inhibitor, AZD6244, there was no additive benefit over either agent alone. This indicates that metformin may have therapeutic utility when combined with inhibitors of the PI3K pathway. In an on-going single-arm, open-label phase II trial at M.D. Anderson Cancer Center of RAD001 (10 mg daily) in combination with letrozole (2.5 mg daily), 9 of the 35 evaluable patients on trial were also using metformin (4 were

on metformin prior to study entry for diabetes, 5 started metformin while on trial for RAD001-induced hyperglycemia). Interestingly, metformin users had a substantially improved clinical benefit rate (CBR) and objective response rate (ORR) (78% and 44%) compared to the 26 metformin non-users on the study, with a CBR and ORR of 39% and 12% in that group. Of the four complete responders on trial, three occurred in the metformin group. Toxicities in patients taking metformin were not significantly different to those not taking metformin.

Metformin may also be combined with cytotoxic agents as a potential chemosensitizer. It was recently demonstrated that metformin potentiates the effects of paclitaxel in endometrial cancer cells through modulation of the mTOR pathway and cell cycle progression (96). These effects may be due in part to metformin's ability to down-regulate glyoxalase I (GloI) expression, an enzyme involved in glycometabolism that is abundant in tumor tissues and has been associated with chemoresistance (114).

Furthermore, our observations may also provide a rationale for use of metformin in several other cancer types that have a high incidence of K-Ras mutations such as pancreatic and colorectal cancer. Indeed, in several retrospective studies, metformin use has been associated with a survival advantage in patients with pancreatic cancer (115) and colorectal cancer (116). However, prospective studies are needed to validate these findings.

5. Conclusions

In conclusion, metformin significantly inhibits cell proliferation, induces apoptosis, and decreases tumor growth in preclinical models of endometrial cancer. Metformin appears to be most effective against mutant K-Ras endometrial cancer cells. Metformin inhibits K-Ras signaling by inducing mislocalization of K-Ras from the plasma membrane to the cytoplasm through a process that appears to be AMPK-independent. Metformin's effects on K-Ras may provide added benefit when combined with other targeted agents, notably mTOR inhibitors, to improve responses. This data provides preclinical support for clinical trials using metformin in combination with PI3K targeted agents, specifically in tumors harboring activating K-Ras mutations.

6. References

1. Nathan, D. M., J. B. Buse, M. B. Davidson, R. J. Heine, R. R. Holman, R. Sherwin, and B. Zinman. 2006. Management of hyperglycemia in type 2 diabetes: A consensus algorithm for the initiation and adjustment of therapy: a consensus statement from the American Diabetes Association and the European Association for the Study of Diabetes. Diabetes Care 29:1963-1972.
2. Kourelis, T. V., and R. D. Siegel. 2012. Metformin and cancer: new applications for an old drug. Med Oncol 29:1314-1327.
3. Evans, J. M., L. A. Donnelly, A. M. Emslie-Smith, D. R. Alessi, and A. D. Morris. 2005. Metformin and reduced risk of cancer in diabetic patients. BMJ 330:1304-1305.
4. Landman, G. W., N. Kleefstra, K. J. van Hateren, K. H. Groenier, R. O. Gans, and H. J. Bilo. 2010. Metformin associated with lower cancer mortality in type 2 diabetes: ZODIAC-16. Diabetes Care 33:322-326.
5. Bowker, S. L., S. R. Majumdar, P. Veugelers, and J. A. Johnson. 2006. Increased cancer-related mortality for patients with type 2 diabetes who use sulfonylureas or insulin. Diabetes Care 29:254-258.
6. Currie, C. J., C. D. Poole, and E. A. Gale. 2009. The influence of glucose-lowering therapies on cancer risk in type 2 diabetes. Diabetologia 52:1766-1777.
7. Home, P. D., S. E. Kahn, N. P. Jones, D. Noronha, H. Beck-Nielsen, and G. Viberti. 2010. Experience of malignancies with oral glucose-lowering drugs in

the randomised controlled ADOPT (A Diabetes Outcome Progression Trial) and RECORD (Rosiglitazone Evaluated for Cardiovascular Outcomes and Regulation of Glycaemia in Diabetes) clinical trials. Diabetologia 53:1838-1845.

8. Monami, M., C. Colombi, D. Balzi, I. Dicembrini, S. Giannini, C. Melani, V. Vitale, D. Romano, A. Barchielli, N. Marchionni, C. M. Rotella, and E. Mannucci. 2011. Metformin and cancer occurrence in insulin-treated type 2 diabetic patients. Diabetes Care 34:129-131.

9. Li, D., S. C. Yeung, M. M. Hassan, M. Konopleva, and J. L. Abbruzzese. 2009. Antidiabetic therapies affect risk of pancreatic cancer. Gastroenterology 137:482-488.

10. Bodmer, M., C. Meier, S. Krahenbuhl, S. S. Jick, and C. R. Meier. 2010. Long-term metformin use is associated with decreased risk of breast cancer. Diabetes Care 33:1304-1308.

11. Hosono, K., H. Endo, H. Takahashi, M. Sugiyama, E. Sakai, T. Uchiyama, K. Suzuki, H. Iida, Y. Sakamoto, K. Yoneda, T. Koide, C. Tokoro, Y. Abe, M. Inamori, H. Nakagama, and A. Nakajima. 2010. Metformin suppresses colorectal aberrant crypt foci in a short-term clinical trial. Cancer Prev Res (Phila) 3:1077-1083.

12. Romero, I. L., A. McCormick, K. A. McEwen, S. Park, T. Karrison, S. D. Yamada, S. Pannain, and E. Lengyel. 2012. Relationship of type II diabetes and metformin use to ovarian cancer progression, survival, and chemosensitivity. Obstet Gynecol 119:61-67.

13. Bailey, C. J., and R. C. Turner. 1996. Metformin. N Engl J Med 334:574-579.

14. Werner, E. A., and J. Bell. 1922. The preparation of methylguanidine and of N,N-dimethylguanidine by the interaction of dicyanodiamide and methylammonium and dimethylammonium chlorides respectively. J Chem Soc, Trans 121:1790-1794.

15. Watanabe, C. K. 1918. Studies in the metabolic changes induced by administration of guanidine bases. J Biol Chem 33:253-265.

16. Bailey, C. J., and C. Day. 2004. Metformin: its botanical background. Practical Diabetes Int 21:115-117.

17. Chen, K. K., and R. C. Anderson. 1947. The toxicity and general pharmacology of N1-p-chlorophenyl-N5-isopropyl biguanide. J Pharmacol Exp Ther 91:157-160.

18. Garcia, E. Y. 1950. Flumamine, a new synthetic analgesic and anti-flu drug. J Philipp Med Assoc 26:287-293.

19. Sterne, J. 1957. Du nouveau dan les antidiabetiques. La NN dimethylamine guanyl guanidine (N.N.D.G). Maroc Med 36:1295-1296.

20. Ben Sahra, I., Y. Le Marchand-Brustel, J. F. Tanti, and F. Bost. Metformin in cancer therapy: a new perspective for an old antidiabetic drug? Mol Cancer Ther 9:1092-1099.

21. Viollet, B., B. Guigas, N. Sanz Garcia, J. Leclerc, M. Foretz, and F. Andreelli. 2012. Cellular and molecular mechanisms of metformin: an overview. Clin Sci (Lond) 122:253-270.

22. Pollak, M. 2008. Insulin and insulin-like growth factor signalling in neoplasia. Nat Rev Cancer 8:915-928.

23. Pollak, M. 2010. Metformin and other biguanides in oncology: advancing the research agenda. Cancer Prev Res (Phila) 3:1060-1065.

24. Pollak, M. 2012. Metformin and Pancreatic Cancer: A Clue Requiring Investigation. Clin Cancer Res.

25. Dowling, R. J., M. Zakikhani, I. G. Fantus, M. Pollak, and N. Sonenberg. 2007. Metformin inhibits mammalian target of rapamycin-dependent translation initiation in breast cancer cells. Cancer Res 67:10804-10812.

26. Zakikhani, M., R. J. Dowling, N. Sonenberg, and M. N. Pollak. 2008. The effects of adiponectin and metformin on prostate and colon neoplasia involve activation of AMP-activated protein kinase. Cancer Prev Res (Phila) 1:369-375.

27. Cantrell, L. A., C. Zhou, A. Mendivil, K. M. Malloy, P. A. Gehrig, and V. L. Bae-Jump. Metformin is a potent inhibitor of endometrial cancer cell proliferation--implications for a novel treatment strategy. Gynecol Oncol 116:92-98.

28. Buzzai, M., R. G. Jones, R. K. Amaravadi, J. J. Lum, R. J. DeBerardinis, F. Zhao, B. Viollet, and C. B. Thompson. 2007. Systemic treatment with the antidiabetic drug metformin selectively impairs p53-deficient tumor cell growth. Cancer Res 67:6745-6752.

29. Wang, X. F., J. Y. Zhang, L. Li, and X. Y. Zhao. 2011. Beneficial effects of metformin on primary cardiomyocytes via activation of adenosine monophosphate-activated protein kinase. Chin Med J (Engl) 124:1876-1884.

30. Wang, X. F., J. Y. Zhang, L. Li, X. Y. Zhao, H. L. Tao, and L. Zhang. 2011. Metformin improves cardiac function in rats via activation of AMP-activated protein kinase. Clin Exp Pharmacol Physiol 38:94-101.

31. Gundewar, S., J. W. Calvert, S. Jha, I. Toedt-Pingel, S. Y. Ji, D. Nunez, A. Ramachandran, M. Anaya-Cisneros, R. Tian, and D. J. Lefer. 2009. Activation of AMP-activated protein kinase by metformin improves left ventricular function and survival in heart failure. Circ Res 104:403-411.

32. 1998. Effect of intensive blood-glucose control with metformin on complications in overweight patients with type 2 diabetes (UKPDS 34). UK Prospective Diabetes Study (UKPDS) Group. Lancet 352:854-865.

33. El Messaoudi, S., G. A. Rongen, R. A. de Boer, and N. P. Riksen. 2011. The cardioprotective effects of metformin. Curr Opin Lipidol 22:445-453.

34. Graham, G. G., J. Punt, M. Arora, R. O. Day, M. P. Doogue, J. K. Duong, T. J. Furlong, J. R. Greenfield, L. C. Greenup, C. M. Kirkpatrick, J. E. Ray, P. Timmins, and K. M. Williams. 2011. Clinical pharmacokinetics of metformin. Clin Pharmacokinet 50:81-98.

35. Zhou, M., L. Xia, and J. Wang. 2007. Metformin transport by a newly cloned proton-stimulated organic cation transporter (plasma membrane monoamine transporter) expressed in human intestine. Drug Metab Dispos 35:1956-1962.

36. Tucker, G. T., C. Casey, P. J. Phillips, H. Connor, J. D. Ward, and H. F. Woods. 1981. Metformin kinetics in healthy subjects and in patients with diabetes mellitus. Br J Clin Pharmacol 12:235-246.

37. Timmins, P., S. Donahue, J. Meeker, and P. Marathe. 2005. Steady-state pharmacokinetics of a novel extended-release metformin formulation. Clin Pharmacokinet 44:721-729.

38. Wilcock, C., and C. J. Bailey. 1994. Accumulation of metformin by tissues of the normal and diabetic mouse. Xenobiotica 24:49-57.

39. Bailey, C. J., K. J. Mynett, and T. Page. 1994. Importance of the intestine as a site of metformin-stimulated glucose utilization. Br J Pharmacol 112:671-675.

40. Nies, A. T., H. Koepsell, S. Winter, O. Burk, K. Klein, R. Kerb, U. M. Zanger, D. Keppler, M. Schwab, and E. Schaeffeler. 2009. Expression of organic cation transporters OCT1 (SLC22A1) and OCT3 (SLC22A3) is affected by genetic factors and cholestasis in human liver. Hepatology 50:1227-1240.

41. Shu, Y., S. A. Sheardown, C. Brown, R. P. Owen, S. Zhang, R. A. Castro, A. G. Ianculescu, L. Yue, J. C. Lo, E. G. Burchard, C. M. Brett, and K. M. Giacomini. 2007. Effect of genetic variation in the organic cation transporter 1 (OCT1) on metformin action. J Clin Invest 117:1422-1431.

42. Segal, E. D., A. Yasmeen, M. C. Beauchamp, J. Rosenblatt, M. Pollak, and W. H. Gotlieb. 2011. Relevance of the OCT1 transporter to the antineoplastic effect of biguanides. Biochem Biophys Res Commun 414:694-699.

43. Alnouti, Y., J. S. Petrick, and C. D. Klaassen. 2006. Tissue distribution and ontogeny of organic cation transporters in mice. Drug Metab Dispos 34:477-482.

44. Bodmer, M., C. Meier, S. Krahenbuhl, S. S. Jick, and C. R. Meier. 2008. Metformin, sulfonylureas, or other antidiabetes drugs and the risk of lactic acidosis or hypoglycemia: a nested case-control analysis. Diabetes Care 31:2086-2091.

45. Vivanco, I., and C. L. Sawyers. 2002. The phosphatidylinositol 3-Kinase AKT pathway in human cancer. Nat Rev Cancer 2:489-501.

46. Yuan, T. L., and L. C. Cantley. 2008. PI3K pathway alterations in cancer: variations on a theme. Oncogene 27:5497-5510.

47. Liu, P., H. Cheng, T. M. Roberts, and J. J. Zhao. 2009. Targeting the phosphoinositide 3-kinase pathway in cancer. Nat Rev Drug Discov 8:627-644.

48. Castellano, E., and J. Downward. 2011. RAS Interaction with PI3K: More Than Just Another Effector Pathway. Genes Cancer 2:261-274.

49. Alessi, D. R., M. Deak, A. Casamayor, F. B. Caudwell, N. Morrice, D. G. Norman, P. Gaffney, C. B. Reese, C. N. MacDougall, D. Harbison, A. Ashworth, and M. Bownes. 1997. 3-Phosphoinositide-dependent protein kinase-1 (PDK1): structural and functional homology with the Drosophila DSTPK61 kinase. Curr Biol 7:776-789.

50. Stephens, L., K. Anderson, D. Stokoe, H. Erdjument-Bromage, G. F. Painter, A. B. Holmes, P. R. Gaffney, C. B. Reese, F. McCormick, P. Tempst, J.

Coadwell, and P. T. Hawkins. 1998. Protein kinase B kinases that mediate phosphatidylinositol 3,4,5-trisphosphate-dependent activation of protein kinase B. Science 279:710-714.

51. Sarbassov, D. D., D. A. Guertin, S. M. Ali, and D. M. Sabatini. 2005. Phosphorylation and regulation of Akt/PKB by the rictor-mTOR complex. Science 307:1098-1101.

52. Mendoza, M. C., E. E. Er, and J. Blenis. 2011. The Ras-ERK and PI3K-mTOR pathways: cross-talk and compensation. Trends Biochem Sci 36:320-328.

53. Rodriguez-Viciana, P., P. H. Warne, R. Dhand, B. Vanhaesebroeck, I. Gout, M. J. Fry, M. D. Waterfield, and J. Downward. 1994. Phosphatidylinositol-3-OH kinase as a direct target of Ras. Nature 370:527-532.

54. Kodaki, T., R. Woscholski, B. Hallberg, P. Rodriguez-Viciana, J. Downward, and P. J. Parker. 1994. The activation of phosphatidylinositol 3-kinase by Ras. Curr Biol 4:798-806.

55. Rubio, I., P. Rodriguez-Viciana, J. Downward, and R. Wetzker. 1997. Interaction of Ras with phosphoinositide 3-kinase gamma. Biochem J 326 (Pt 3):891-895.

56. Prior, I. A., and J. F. Hancock. 2011. Ras trafficking, localization and compartmentalized signalling. Semin Cell Dev Biol.

57. Ahearn, I. M., K. Haigis, D. Bar-Sagi, and M. R. Philips. 2012. Regulating the regulator: post-translational modification of RAS. Nat Rev Mol Cell Biol 13:39-51.

58. Wright, L. P., and M. R. Philips. 2006. Thematic review series: lipid posttranslational modifications. CAAX modification and membrane targeting of Ras. J Lipid Res 47:883-891.

59. Hancock, J. F., H. Paterson, and C. J. Marshall. 1990. A polybasic domain or palmitoylation is required in addition to the CAAX motif to localize p21ras to the plasma membrane. Cell 63:133-139.

60. Choy, E., V. K. Chiu, J. Silletti, M. Feoktistov, T. Morimoto, D. Michaelson, I. E. Ivanov, and M. R. Philips. 1999. Endomembrane trafficking of ras: the CAAX motif targets proteins to the ER and Golgi. Cell 98:69-80.

61. Apolloni, A., I. A. Prior, M. Lindsay, R. G. Parton, and J. F. Hancock. 2000. H-ras but not K-ras traffics to the plasma membrane through the exocytic pathway. Mol Cell Biol 20:2475-2487.

62. Goodwin, J. S., K. R. Drake, C. Rogers, L. Wright, J. Lippincott-Schwartz, M. R. Philips, and A. K. Kenworthy. 2005. Depalmitoylated Ras traffics to and from the Golgi complex via a nonvesicular pathway. J Cell Biol 170:261-272.

63. Silvius, J. R., P. Bhagatji, R. Leventis, and D. Terrone. 2006. K-ras4B and prenylated proteins lacking "second signals" associate dynamically with cellular membranes. Mol Biol Cell 17:192-202.

64. Rodriguez-Viciana, P., P. H. Warne, A. Khwaja, B. M. Marte, D. Pappin, P. Das, M. D. Waterfield, A. Ridley, and J. Downward. 1997. Role of phosphoinositide 3-OH kinase in cell transformation and control of the actin cytoskeleton by Ras. Cell 89:457-467.

65. Li, W., T. Zhu, and K. L. Guan. 2004. Transformation potential of Ras isoforms correlates with activation of phosphatidylinositol 3-kinase but not ERK. J Biol Chem 279:37398-37406.

66. Sheng, H., J. Shao, and R. N. DuBois. 2001. Akt/PKB activity is required for Ha-Ras-mediated transformation of intestinal epithelial cells. J Biol Chem 276:14498-14504.

67. Lim, K. H., and C. M. Counter. 2005. Reduction in the requirement of oncogenic Ras signaling to activation of PI3K/AKT pathway during tumor maintenance. Cancer Cell 8:381-392.

68. Yu, C. F., Z. X. Liu, and L. G. Cantley. 2002. ERK negatively regulates the epidermal growth factor-mediated interaction of Gab1 and the phosphatidylinositol 3-kinase. J Biol Chem 277:19382-19388.

69. Hoeflich, K. P., C. O'Brien, Z. Boyd, G. Cavet, S. Guerrero, K. Jung, T. Januario, H. Savage, E. Punnoose, T. Truong, W. Zhou, L. Berry, L. Murray, L. Amler, M. Belvin, L. S. Friedman, and M. R. Lackner. 2009. In vivo antitumor activity of MEK and phosphatidylinositol 3-kinase inhibitors in basal-like breast cancer models. Clin Cancer Res 15:4649-4664.

70. Zoncu, R., A. Efeyan, and D. M. Sabatini. 2011. mTOR: from growth signal integration to cancer, diabetes and ageing. Nat Rev Mol Cell Biol 12:21-35.

71. Carriere, A., Y. Romeo, H. A. Acosta-Jaquez, J. Moreau, E. Bonneil, P. Thibault, D. C. Fingar, and P. P. Roux. 2011. ERK1/2 phosphorylate Raptor to promote Ras-dependent activation of mTOR complex 1 (mTORC1). J Biol Chem 286:567-577.

72. Di Nicolantonio, F., S. Arena, J. Tabernero, S. Grosso, F. Molinari, T. Macarulla, M. Russo, C. Cancelliere, D. Zecchin, L. Mazzucchelli, T. Sasazuki, S. Shirasawa, M. Geuna, M. Frattini, J. Baselga, M. Gallicchio, S. Biffo, and A. Bardelli. 2010. Deregulation of the PI3K and KRAS signaling pathways in human cancer cells determines their response to everolimus. J Clin Invest 120:2858-2866.

73. Kinkade, C. W., M. Castillo-Martin, A. Puzio-Kuter, J. Yan, T. H. Foster, H. Gao, Y. Sun, X. Ouyang, W. L. Gerald, C. Cordon-Cardo, and C. Abate-Shen. 2008. Targeting AKT/mTOR and ERK MAPK signaling inhibits hormone-refractory prostate cancer in a preclinical mouse model. J Clin Invest 118:3051-3064.

74. Engelman, J. A., L. Chen, X. Tan, K. Crosby, A. R. Guimaraes, R. Upadhyay, M. Maira, K. McNamara, S. A. Perera, Y. Song, L. R. Chirieac, R. Kaur, A. Lightbown, J. Simendinger, T. Li, R. F. Padera, C. Garcia-Echeverria, R. Weissleder, U. Mahmood, L. C. Cantley, and K. K. Wong. 2008. Effective use of PI3K and MEK inhibitors to treat mutant Kras G12D and PIK3CA H1047R murine lung cancers. Nat Med 14:1351-1356.

75. Haagensen, E. J., S. Kyle, G. S. Beale, R. J. Maxwell, and D. R. Newell. 2012. The synergistic interaction of MEK and PI3K inhibitors is modulated by mTOR inhibition. Br J Cancer 106:1386-1394.

76. Siegel, R., E. Ward, O. Brawley, and A. Jemal. Cancer statistics, 2011: the impact of eliminating socioeconomic and racial disparities on premature cancer deaths. CA Cancer J Clin 61:212-236.

77. Calle, E. E., C. Rodriguez, K. Walker-Thurmond, and M. J. Thun. 2003. Overweight, obesity, and mortality from cancer in a prospectively studied cohort of U.S. adults. N Engl J Med 348:1625-1638.

78. Jiralerspong, S., S. L. Palla, S. H. Giordano, F. Meric-Bernstam, C. Liedtke, C. M. Barnett, L. Hsu, M. C. Hung, G. N. Hortobagyi, and A. M. Gonzalez-Angulo. 2009. Metformin and pathologic complete responses to neoadjuvant chemotherapy in diabetic patients with breast cancer. J Clin Oncol 27:3297-3302.

79. Mutter, G. L., M. C. Lin, J. T. Fitzgerald, J. B. Kum, J. P. Baak, J. A. Lees, L. P. Weng, and C. Eng. 2000. Altered PTEN expression as a diagnostic marker for the earliest endometrial precancers. J Natl Cancer Inst 92:924-930.

80. Maxwell, G. L., J. I. Risinger, C. Gumbs, H. Shaw, R. C. Bentley, J. C. Barrett, A. Berchuck, and P. A. Futreal. 1998. Mutation of the PTEN tumor suppressor gene in endometrial hyperplasias. Cancer Res 58:2500-2503.

81. Oda, K., D. Stokoe, Y. Taketani, and F. McCormick. 2005. High frequency of coexistent mutations of PIK3CA and PTEN genes in endometrial carcinoma. Cancer Res 65:10669-10673.

82. Prat, J. 2004. Prognostic parameters of endometrial carcinoma. Hum Pathol 35:649-662.

83. Okuda, T., A. Sekizawa, Y. Purwosunu, M. Nagatsuka, M. Morioka, M. Hayashi, and T. Okai. 2010. Genetics of endometrial cancers. Obstet Gynecol Int 2010:984013.

84. Lax, S. F., B. Kendall, H. Tashiro, R. J. Slebos, and L. Hedrick. 2000. The frequency of p53, K-ras mutations, and microsatellite instability differs in uterine endometrioid and serous carcinoma: evidence of distinct molecular genetic pathways. Cancer 88:814-824.

85. Oda, K., J. Okada, L. Timmerman, P. Rodriguez-Viciana, D. Stokoe, K. Shoji, Y. Taketani, H. Kuramoto, Z. A. Knight, K. M. Shokat, and F. McCormick. 2008. PIK3CA cooperates with other phosphatidylinositol 3'-kinase pathway mutations to effect oncogenic transformation. Cancer Res 68:8127-8136.

86. Llobet, D., J. Pallares, A. Yeramian, M. Santacana, N. Eritja, A. Velasco, X. Dolcet, and X. Matias-Guiu. 2009. Molecular pathology of endometrial carcinoma: practical aspects from the diagnostic and therapeutic viewpoints. J Clin Pathol 62:777-785.

87. Samarnthai, N., K. Hall, and I. T. Yeh. 2010. Molecular profiling of endometrial malignancies. Obstet Gynecol Int 2010:162363.

88. Matias-Guiu, X., L. Catasus, E. Bussaglia, H. Lagarda, A. Garcia, C. Pons, J. Munoz, R. Arguelles, P. Machin, and J. Prat. 2001. Molecular pathology of endometrial hyperplasia and carcinoma. Hum Pathol 32:569-577.

89. Prat, J., A. Gallardo, M. Cuatrecasas, and L. Catasus. 2007. Endometrial carcinoma: pathology and genetics. Pathology 39:72-87.

90. Sasaki, H., H. Nishii, H. Takahashi, A. Tada, M. Furusato, Y. Terashima, G. P. Siegal, S. L. Parker, M. F. Kohler, A. Berchuck, and et al. 1993. Mutation of the Ki-ras protooncogene in human endometrial hyperplasia and carcinoma. Cancer Res 53:1906-1910.

91. Mirabelli-Primdahl, L., R. Gryfe, H. Kim, A. Millar, C. Luceri, D. Dale, E. Holowaty, B. Bapat, S. Gallinger, and M. Redston. 1999. Beta-catenin mutations are specific for colorectal carcinomas with microsatellite instability but occur in endometrial carcinomas irrespective of mutator pathway. Cancer Res 59:3346-3351.

92. Bansal, N., V. Yendluri, and R. M. Wenham. 2009. The molecular biology of endometrial cancers and the implications for pathogenesis, classification, and targeted therapies. Cancer Control 16:8-13.

93. Morrison, C., V. Zanagnolo, N. Ramirez, D. E. Cohn, N. Kelbick, L. Copeland, G. L. Maxwell, and J. M. Fowler. 2006. HER-2 is an independent prognostic factor in endometrial cancer: association with outcome in a large cohort of surgically staged patients. J Clin Oncol 24:2376-2385.

94. Libby, G., L. A. Donnelly, P. T. Donnan, D. R. Alessi, A. D. Morris, and J. M. Evans. 2009. New users of metformin are at low risk of incident cancer: a cohort study among people with type 2 diabetes. Diabetes Care 32:1620-1625.

95. Decensi, A., M. Puntoni, P. Goodwin, M. Cazzaniga, A. Gennari, B. Bonanni, and S. Gandini. Metformin and cancer risk in diabetic patients: a systematic review and meta-analysis. Cancer Prev Res (Phila) 3:1451-1461.

96. Hanna, R. K., C. Zhou, K. M. Malloy, L. Sun, Y. Zhong, P. A. Gehrig, and V. L. Bae-Jump. 2012. Metformin potentiates the effects of paclitaxel in endometrial cancer cells through inhibition of cell proliferation and modulation of the mTOR pathway. Gynecol Oncol 125:458-469.

97. Kim, T. H., J. Wang, K. Y. Lee, H. L. Franco, R. R. Broaddus, J. P. Lydon, J. W. Jeong, and F. J. Demayo. 2010. The Synergistic Effect of Conditional Pten Loss and Oncogenic K-ras Mutation on Endometrial Cancer Development Occurs via Decreased Progesterone Receptor Action. J Oncol 2010:139087.

98. Iwanaga, K., Y. Yang, M. G. Raso, L. Ma, A. E. Hanna, N. Thilaganathan, S. Moghaddam, C. M. Evans, H. Li, W. W. Cai, M. Sato, J. D. Minna, H. Wu, C. J. Creighton, F. J. Demayo, Wistuba, II, and J. M. Kurie. 2008. Pten inactivation accelerates oncogenic K-ras-initiated tumorigenesis in a mouse model of lung cancer. Cancer Res 68:1119-1127.

99. Thor, A., and S. M. Anderson. 2011. Preclinical studies of metformin action in breast cancer. ASCO Educational Book:46-49.

100. Reagan-Shaw, S., M. Nihal, and N. Ahmad. 2008. Dose translation from animal to human studies revisited. FASEB J 22:659-661.

101. Velho, S., C. Oliveira, A. Ferreira, A. C. Ferreira, G. Suriano, S. Schwartz, Jr., A. Duval, F. Carneiro, J. C. Machado, R. Hamelin, and R. Seruca. 2005. The prevalence of PIK3CA mutations in gastric and colon cancer. Eur J Cancer 41:1649-1654.

102. Algire, C., O. Moiseeva, X. Deschenes-Simard, L. Amrein, L. Petruccelli, E. Birman, B. Viollet, G. Ferbeyre, and M. N. Pollak. 2012. Metformin Reduces Endogenous Reactive Oxygen Species and Associated DNA Damage. Cancer Prev Res (Phila).

103. Malki, A., and A. Youssef. 2011. Antidiabetic drug metformin induces apoptosis in human MCF breast cancer via targeting ERK signaling. Oncol Res 19:275-285.

104. Bivona, T. G., S. E. Quatela, B. O. Bodemann, I. M. Ahearn, M. J. Soskis, A. Mor, J. Miura, H. H. Wiener, L. Wright, S. G. Saba, D. Yim, A. Fein, I. Perez de Castro, C. Li, C. B. Thompson, A. D. Cox, and M. R. Philips. 2006. PKC regulates a farnesyl-electrostatic switch on K-Ras that promotes its association with Bcl-XL on mitochondria and induces apoptosis. Mol Cell 21:481-493.

105. Eisenberg, S., K. Giehl, Y. I. Henis, and M. Ehrlich. 2008. Differential interference of chlorpromazine with the membrane interactions of oncogenic K-Ras and its effects on cell growth. J Biol Chem 283:27279-27288.

106. Sajan, M. P., G. Bandyopadhyay, A. Miura, M. L. Standaert, S. Nimal, S. L. Longnus, E. Van Obberghen, I. Hainault, F. Foufelle, R. Kahn, U. Braun, M. Leitges, and R. V. Farese. 2010. AICAR and metformin, but not exercise, increase muscle glucose transport through AMPK-, ERK-, and PDK1-dependent activation of atypical PKC. Am J Physiol Endocrinol Metab 298:E179-192.

107. Vander Heiden, M. G., L. C. Cantley, and C. B. Thompson. 2009. Understanding the Warburg effect: the metabolic requirements of cell proliferation. Science 324:1029-1033.

108. Neuzil, J., J. Rohlena, and L. F. Dong. 2012. K-Ras and mitochondria: dangerous liaisons. Cell Res 22:285-287.

109. Hu, Y., W. Lu, G. Chen, P. Wang, Z. Chen, Y. Zhou, M. Ogasawara, D. Trachootham, L. Feng, H. Pelicano, P. J. Chiao, M. J. Keating, G. Garcia-Manero, and P. Huang. 2012. K-ras(G12V) transformation leads to mitochondrial dysfunction and a metabolic switch from oxidative phosphorylation to glycolysis. Cell Res 22:399-412.

110. Ben Sahra, I., Y. Le Marchand-Brustel, J. F. Tanti, and F. Bost. 2010. Metformin in cancer therapy: a new perspective for an old antidiabetic drug? Mol Cancer Ther 9:1092-1099.

111. El-Mir, M. Y., V. Nogueira, E. Fontaine, N. Averet, M. Rigoulet, and X. Leverve. 2000. Dimethylbiguanide inhibits cell respiration via an indirect effect targeted on the respiratory chain complex I. J Biol Chem 275:223-228.

112. Ben Sahra, I., K. Laurent, S. Giuliano, F. Larbret, G. Ponzio, P. Gounon, Y. Le Marchand-Brustel, S. Giorgetti-Peraldi, M. Cormont, C. Bertolotto, M. Deckert, P. Auberger, J. F. Tanti, and F. Bost. 2010. Targeting cancer cell metabolism: the combination of metformin and 2-deoxyglucose induces p53-dependent apoptosis in prostate cancer cells. Cancer Res 70:2465-2475.

113. Dedes, K. J., D. Wetterskog, A. Ashworth, S. B. Kaye, and J. S. Reis-Filho. Emerging therapeutic targets in endometrial cancer. Nat Rev Clin Oncol 8:261-271.

114. Dong, L., Q. Zhou, Z. Zhang, Y. Zhu, T. Duan, and Y. Feng. 2012. Metformin sensitizes endometrial cancer cells to chemotherapy by repressing glyoxalase I expression. J Obstet Gynaecol Res.

115. Sadeghi, N., J. L. Abbruzzese, S. C. Yeung, M. Hassan, and D. Li. 2012. Metformin Use Is Associated with Better Survival of Diabetic Patients with Pancreatic Cancer. Clin Cancer Res.

116. Garrett, C. R., H. M. Hassabo, N. A. Bhadkamkar, S. Wen, V. Baladandayuthapani, B. K. Kee, C. Eng, and M. M. Hassan. 2012. Survival advantage observed with the use of metformin in patients with type II diabetes and colorectal cancer. Br J Cancer.

VITA

David Alberto Iglesias was born in Cordoba, Spain on October 8th, 1981, the son of Jesus and Ana M. Iglesias. David graduated from the University of Florida in 2003 earning a Bachelor's of Science in Biomedical Sciences while participating in the Junior Honors Medical Program. He went on to receive a Doctor of Medicine degree from the University of Florida College of Medicine in 2006. David completed a residency in Obstetrics and Gynecology also at the University of Florida and Shands Hospital. Following the completion of residency, David was accepted into the gynecologic oncology fellowship program at the University of Texas, M.D. Anderson Cancer Center. During the first two years of his fellowship, he decided to receive formal training in cancer biology research through the University of Texas Graduate School of Biomedical Sciences. After the completion of two additional years of clinical training, he is anticipated to complete the fellowship in June 2014.